

# Towards an effective-action approach to fermion-loop corrections \*

W. Beenakker<sup>1</sup>, A.P. Chapovsky<sup>2</sup>, A. Kanaki<sup>3</sup>,  
C.G. Papadopoulos<sup>3,4†</sup>, R. Pittau<sup>5‡</sup>

<sup>1</sup> Theoretical Physics, Univ. of Nijmegen, NL-6500 GL Nijmegen, The Netherlands

<sup>2</sup> Institut für Theoretische Physik E, RWTH Aachen, D-52056 Aachen, Germany

<sup>3</sup> Institute of Nuclear Physics, NCSR “Demokritos”, 15310, Athens, Greece

<sup>4</sup> Theory Division, CERN, CH-1211, Geneva, Switzerland

<sup>5</sup> Dipartimento di Fisica Teorica, Università di Torino, Italy  
and INFN sezione di Torino, Italy

## Abstract

We present a study of the effective action approach to incorporate higher-order effects in  $e^+e^- \rightarrow n$  fermions. In its minimal version, the effective action approach is found to exhibit problems with unitarity and high-energy behaviour. We identify the origin of these problems by investigating the zero-mode solutions of the Ward Identities. A numerical analysis of the importance of the zero-mode solutions is presented for four-fermion production processes.

---

\*Work supported by the European Union under contract HPRN-CT-2000-00149

†Financially supported by EU contract HPMF-CT-2002-01622

‡Financially supported by MIUR under contract 2001023713-006

# 1 Introduction

Multi-fermion production processes constitute one of the most important classes of reactions at electron–positron colliders [1]. Through high-precision studies of these reactions valuable information is gained on the electroweak parameters, on the interactions between the electroweak gauge bosons and on the mechanism of electroweak symmetry breaking. High-precision studies of this kind demand a precise description of the physics of the unstable gauge bosons that occur during the intermediate stages of the reactions. One problematic, though crucial ingredient for achieving such a description is the incorporation of the associated finite-width effects. To this end one has to resum the relevant gauge-boson self-energies, which results in a mixing of different orders of perturbation theory and thereby jeopardizes gauge invariance. Since the high precision of the experiments has to be matched by the precision of the theoretical predictions, both an adequate treatment of the finite-width effects and a sufficiently accurate perturbative expansion are required. The clash between resummation and perturbative expansion can therefore not be ignored.

A procedure to overcome this dilemma has been proposed several years ago and is known under the name of Fermion Loop (FL) scheme [2, 3, 4, 5]. In this scheme a resummation of all one-loop fermionic corrections to gauge-boson self-energies is performed. In order to account for a consistent and gauge-invariant treatment, the one-particle-irreducible (1PI) fermionic one-loop corrections to the other  $n$ -point gauge-boson functions (with  $n \geq 3$ ) are included as well. The FL scheme essentially involves the closed subset of all  $\mathcal{O}([N_C^f \alpha/\pi]^n)$  contributions to a given physical process, with  $N_C^f$  denoting the colour degeneracy of fermion  $f$ , and as such it is manifestly consistent. The reason for singling out the fermionic one-loop corrections lies in the fact that the unstable gauge bosons decay exclusively into fermions at lowest order. The FL scheme has proven particularly successful in dealing with four-fermion production processes. Although in the beginning it merely served the purpose of a consistent scheme for including the width of the  $W$  boson [2], which is closely related to the imaginary part of the  $W$ -boson self-energy, very soon people realized that it can also accommodate the resummation of the real parts of the gauge-boson self-energies [3, 4], which are responsible for the running of the couplings with energy.

Unfortunately there are several limitations related to the FL scheme. First of all, it is clearly a partial answer to the problem of resumming higher-order corrections. It is restricted to closed fermion loops, which means that bosonic contributions are ignored. Several methods have been proposed to overcome this limitation. The most efficient one is the so-called pole-scheme [6], which

amounts to a systematic expansion of the matrix elements around the complex poles in the unstable-particle propagators. In leading order of this expansion the radiative corrections involve the *full* set of one-loop corrections to on-shell gauge-boson production and decay (factorizable corrections) [7, 8], as well as soft-photon corrections that take into account the fact that the production and decay stages of the reaction do not proceed independently (non-factorizable corrections) [9]. However, in reactions with several intermediate unstable gauge bosons, like e.g. six-fermion production, it becomes rather awkward to perform the complete pole-scheme expansion [7]. Secondly, even though the FL scheme is conceptually straightforward, it becomes more and more involved computationally once one goes beyond the four-fermion production processes. For instance, for general multi-fermion production processes one has to consider the complete set of fermionic one-loop corrections to the 1PI four-point gauge-boson functions, five-point gauge-boson functions, and so on.

In the meantime a novel proposal has emerged, as described in the paper by Beenakker, Berends and Chapovsky [10], abbreviated as BBC from now on. Their proposal consists essentially in a re-arrangement of the expansion of the effective action of the theory, which is usually performed in terms of the 1PI Feynman amplitudes, in such a way that the new expansion is manifestly gauge invariant. Restricting ourselves, for simplicity, to a pure  $SU(N)$  gauge theory, the expansion looks like

$$\begin{aligned}
\mathcal{S}_{NL} = & \int d^4x d^4y G_2(x, y) \text{Tr} [U(y, x) \mathbf{F}_{\mu\nu}(x) U(x, y) \mathbf{F}^{\mu\nu}(y)] \\
& + \int d^4x d^4y d^4z G_3(x, y, z) \text{Tr} [U(z, x) \mathbf{F}_{\mu\nu}(x) U(x, y) \mathbf{F}^{\mu\rho}(y) U(y, z) \mathbf{F}^{\nu\rho}(z)] \\
& + \dots
\end{aligned} \tag{1}$$

Here the trace has to be taken in group space and  $\mathbf{F}_{\mu\nu} \equiv \frac{i}{g} [D_\mu, D_\nu]$  is the  $SU(N)$  field-strength tensor, expressed in terms of the covariant derivative  $D_\mu$  and the gauge coupling  $g$ . The operator  $U(x, y)$  is a path-ordered exponential, which carries the gauge transformation from one space-time point to the other (see Section 2 for a more detailed definition). In Eq.(1) each gauge-invariant non-local operator is multiplied by an appropriate space-time function  $G_i$  that can, in principle, be computed within perturbation theory. In the context of fermionic loop effects, the various terms in Eq.(1) can be viewed as the result of integrating out the fermions in the functional integral, resulting in a kind of non-local lagrangian for gauge-boson interactions. The minimum number of gauge bosons that participate in the effective interaction is two for the first term of Eq.(1), three for the second term, and so on. Note, however, that each term

will also generate all higher  $n$ -point interactions, through the expansion of the path-ordered exponentials (see Section 2). These higher  $n$ -point interactions are essential for achieving gauge invariance for the individual terms of Eq.(1). Since all ingredients for the resummation of the gauge-boson self-energies are contained in the first (self-energy-like) term of Eq.(1), it was proposed in the BBC approach to truncate the series at this first term. In this way an economic gauge-invariant framework for resumming self-energies is obtained, leading to matrix elements that satisfy all relevant Ward Identities. Two questions remain open at this point: “How should one match the space-time function  $G_2$  with the actual fermion-loop corrections?” and “Is gauge invariance sufficient for obtaining well-behaved matrix elements?”.

In this paper we undertake the effort to confront the BBC idea with actual calculations, addressing in this way the two outstanding questions. In Section 2 we consider the matching aspect. We introduce the set of gauge-invariant operators that is relevant for an exact description of fermion-loop corrections in the two-point gauge-boson sector of the Standard Model (SM), involving both electroweak gauge bosons and Higgs fields. In Section 3 we identify and analyse a problem with the high-energy behaviour of the matrix element for the reaction  $e^+e^- \rightarrow W^+W^-$ . This problem is related to the non-unitary character of the truncation in the BBC approach. We pinpoint the source of the problem to be in the zero-mode solutions of the Ward Identities, like the second term of Eq.(1), which are absent in the BBC approach. In Section 4 the set-up of the calculations as well as the numerical results are presented and discussed. Particular emphasis is put on an investigation of the numerical importance of the zero-mode solutions. Finally, the paper is concluded with a few appendices, where all relevant information pertaining to the non-local Feynman rules, renormalization schemes and the unitarity problem in the reaction  $e^+e^- \rightarrow W^+W^-$  can be found.

## 2 The effective-action approach

### 2.1 Notation and conventions

Before turning our attention to the non-local lagrangian, we first introduce the notation and conventions that will be used throughout the remainder of this paper. In the SM there are four gauge fields, the  $SU(2)_L$  (isospin) gauge fields  $W_\mu^a$  ( $a = 1, 2, 3$ ) and the  $U(1)_Y$  (hypercharge) gauge field  $B_\mu$ . The corresponding field-strength tensors are given by

$$\mathbf{F}_{\mu\nu} = \partial_\mu \mathbf{W}_\nu - \partial_\nu \mathbf{W}_\mu - i g_2 [\mathbf{W}_\mu, \mathbf{W}_\nu], \quad B_{\mu\nu} = \partial_\mu B_\nu - \partial_\nu B_\mu, \quad (2)$$

using the shorthand notations

$$\mathbf{F}_{\mu\nu} \equiv T^a F_{\mu\nu}^a, \quad \mathbf{W}_\mu \equiv T^a W_\mu^a. \quad (3)$$

The  $SU(2)_L$  and  $U(1)_Y$  gauge couplings are indicated by  $g_2$  and  $g_1$ , respectively, and the  $SU(2)_L$  generators  $T^a$  can be expressed in terms of the standard Pauli spin matrices  $\sigma^a$  ( $a = 1, 2, 3$ ) according to  $T^a = \sigma^a/2$ . These generators obey the commutation relation  $[T^a, T^b] = i \epsilon^{abc} T^c$ , with the  $SU(2)$  structure constant  $\epsilon^{abc}$  given by

$$\epsilon^{abc} = \begin{cases} +1 & \text{if } (a, b, c) = \text{even permutation of } (1, 2, 3) \\ -1 & \text{if } (a, b, c) = \text{odd permutation of } (1, 2, 3) \\ 0 & \text{else} \end{cases}. \quad (4)$$

The physically observable gauge-boson states are given by

$$W_\mu^\pm = \frac{1}{\sqrt{2}} (W_\mu^1 \mp i W_\mu^2), \quad Z_\mu = c_w W_\mu^3 + s_w B_\mu, \quad A_\mu = c_w B_\mu - s_w W_\mu^3, \quad (5)$$

for the  $W^\pm$  bosons,  $Z$  boson and photon, respectively. Here  $c_w = g_2/\sqrt{g_1^2 + g_2^2}$  and  $s_w = \sqrt{1 - c_w^2}$  are the cosine and sine of the weak mixing angle. The electromagnetic coupling constant can be obtained from  $g_1$  and  $g_2$  according to  $e = \sqrt{4\pi\alpha} = g_1 g_2 / \sqrt{g_1^2 + g_2^2}$ .

Since we want to discuss the entire gauge-boson sector, we also need to introduce the would-be Goldstone bosons  $\phi^\pm$  and  $\chi$  that are intimately linked to the longitudinal degrees of freedom of the massive  $W^\pm$  and  $Z$  gauge bosons. To this end we introduce the ( $Y = 1$ ) Higgs doublet

$$\Phi(x) = \begin{pmatrix} \phi^+(x) \\ [v + H(x) + i\chi(x)]/\sqrt{2} \end{pmatrix} \quad (6)$$

and the corresponding covariant derivative

$$D_\mu = \partial_\mu - i g_2 \mathbf{W}_\mu + i \frac{g_1}{2} B_\mu. \quad (7)$$

Here  $v/\sqrt{2}$  is the non-zero vacuum expectation value of the Higgs field, yielding  $M_W = v g_2/2$  and  $M_Z = M_W/c_w$  for the masses of the  $W$  and  $Z$  bosons in this convention.

A few more definitions are needed for the description of the fermionic corrections to the various self-energies in the gauge-boson sector of the SM. A generic SM fermion will be indicated by  $f$  and its isospin partner by  $f'$ . The  $SU(3)_C$  colour factor, mass, electromagnetic charge and isospin of the fermion  $f$  are denoted by  $N_C^f$ ,  $m_f$ ,  $eQ_f$  and  $I_f^3$ , respectively. Finally, the hypercharge of the left-handed and right-handed fermions is denoted by  $Y_f^L$  and  $Y_f^R$ , respectively.

## 2.2 The non-local lagrangian

Following Ref. [10] we introduce an effective action that includes all relevant two-point interactions in the gauge-boson sector, involving both gauge-boson and Higgs fields. This *non-local* lagrangian can be written as

$$\begin{aligned}
\mathcal{S}_{\text{NL}} = & -\frac{1}{4} \int d^4x d^4y \Sigma_1(x-y) B_{\mu\nu}(x) B^{\mu\nu}(y) \\
& -\frac{1}{2} \int d^4x d^4y \Sigma_2(x-y) \text{Tr} [U_2(y,x) \mathbf{F}_{\mu\nu}(x) U_2(x,y) \mathbf{F}^{\mu\nu}(y)] \\
& -\frac{2}{v^2} \frac{g_1}{g_2} \int d^4x d^4y \Sigma_3(x-y) [\Phi^\dagger(x) \mathbf{F}_{\mu\nu}(x) \Phi(x)] B^{\mu\nu}(y) \\
& -\frac{4}{v^4} \int d^4x d^4y \Sigma_4(x-y) [\Phi^\dagger(x) \mathbf{F}_{\mu\nu}(x) \Phi(x)] [\Phi^\dagger(y) \mathbf{F}^{\mu\nu}(y) \Phi(y)] \\
& + \int d^4x d^4y \Sigma_5(x-y) [D_\mu \Phi(x)]^\dagger U_2(x,y) U_1(x,y) D^\mu \Phi(y) \\
& + \frac{2}{v^2} \int d^4x d^4y \Sigma_6(x-y) [\Phi^\dagger(x) D_\mu \Phi(x)]^\dagger [\Phi^\dagger(y) D^\mu \Phi(y)]. \tag{8}
\end{aligned}$$

A few comments and definitions are in order here. First of all, the arguments of the non-local coefficients  $\Sigma_1(x-y), \dots, \Sigma_6(x-y)$  follow directly from translational invariance. Furthermore, the trace appearing in the 2nd term has to be taken in  $SU(2)_L$  group space. Finally, the path-ordered exponentials for the  $SU(2)_L$  and  $U(1)_Y$  gauge groups are defined according to

$$\begin{aligned}
U_2(x,y) &= Pexp \left[ -ig_2 \int_x^y \mathbf{W}_\mu(\omega) d\omega^\mu \right] \\
U_1(x,y) &= Pexp \left[ +ig_1 \frac{Y}{2} \int_x^y B_\mu(\omega) d\omega^\mu \right], \tag{9}
\end{aligned}$$

where  $Y = 1$  for the Higgs doublet and  $d\omega^\mu$  is the element of integration along some path  $\Omega(x,y)$  that connects the points  $x$  and  $y$ . According to Ref. [10] the path is defined in such a way that it does not involve closed loops, i.e. the null path  $\Omega(x,x)$  always has zero length. Moreover, the choice of path should be such that it gives rise to path-ordered exponentials with specific properties under differentiation.

Let us repeat the main points of the BBC approach:

- The BBC effective action in Eq.(8) is gauge invariant by construction.
- Through the expansion of the path-ordered exponentials, the effective action incorporates a set of higher 3-,4-, $\dots$ ,  $n$ -point functions that automatically satisfy the Ward Identities of the theory. A complete set of three-point Feynman rules based on Eq.(8) is given in Appendix A.

- A set of unknown coefficients  $\Sigma_1, \dots, \Sigma_6$  is introduced.

There are several ways to determine the unknown coefficients. Some simplified expressions, corresponding to existing ad hoc approximations for incorporating finite-width effects, have already been presented in Ref. [10]. These expressions involve only a partial resummation of the fermionic corrections, in contrast to the full 1PI resummation that is performed in the FL scheme. In this paper we investigate how the unknown BBC coefficients can be matched with the well-established two-point fermion-loop contributions in the SM. By doing so, we obtain an exact correspondence between the SM and the effective BBC action for all reactions that involve at most two-point interactions among the gauge bosons. For reactions that involve interactions among three gauge bosons or more, the effective BBC approach provides us with a minimal set of contributions that is required for satisfying all relevant Ward Identities. Although this approximation cannot be identical to that of the FL scheme, one might anticipate that it provides a much more economic approach to multi-fermion production processes. After all, in the FL scheme one has to perform a complete calculation of the SM  $n$ -point functions with three or more external gauge bosons, which constitutes a rather intensive and costly procedure. On the other hand, by truncating the non-local action at ‘two-point order’ several parts of the higher-order corrections are neglected. It is therefore important to understand to what extent one can trust such an approximation.

### 2.3 The matching procedure

In order to set up the framework of our studies, we present in this subsection the matching procedure, i.e. the determination of the non-local coefficients  $\Sigma_1, \dots, \Sigma_6$ . Using the knowledge of all two-point functions in the FL scheme (see Appendix B), we can perform the first level of matching: mapping the unrenormalized self-energies directly onto the non-local coefficients. The second level of matching, between the so-obtained non-local matrix elements/cross sections and the explicit experimental observables, should take care of any necessary redefinition (renormalization) of couplings and masses.

As can be seen from Appendix B, we indeed need all six non-local operators in Eq.(8) in order to match the six independent gauge-boson self-energies (after tadpole renormalization). The 1st, 2nd and 5th operators in Eq.(8) are non-local extensions of terms in the local SM lagrangian. They take care of all UV-divergent terms present in the fermionic one-loop self-energies. The remaining three operators are higher dimensional ( $\dim > 4$ ). The corresponding coefficients

are finite, as expected for a renormalizable theory, and can be viewed as non-local versions of the oblique  $S$ -,  $T$ - and  $U$ -parameters of Peskin and Takeuchi [11]. These operators are required for achieving an explicit breaking of the global isospin symmetry among the  $SU(2)$  gauge bosons, usually referred to as custodial  $SU(2)$  symmetry [12]. After all, also the loop effects in the SM explicitly break this global symmetry as a result of hypercharge interactions and specific fermion-mass effects.

Below we list the results for the first level of matching of the coefficients  $\tilde{\Sigma}_1, \dots, \tilde{\Sigma}_6$ , which represent the Fourier transforms of the non-local coefficients  $\Sigma_1, \dots, \Sigma_6$  appearing in Eq.(8). These results will be expressed in terms of the transverse and longitudinal self-energy functions  $\Sigma_T^{V_1 V_2}(s)$  and  $\Sigma_L^{V_1 V_2}(s)$ , where  $V_{1,2} = \gamma, Z, W$  and  $s$  represents the square of the momentum at which the self-energies are evaluated. The explicit expressions for these functions can be found in Appendix B in Eqs.(61)–(64).

The transverse, pure hypercharge coefficient  $\tilde{\Sigma}_1$  can be obtained through the relation

$$\begin{aligned} \tilde{\Sigma}_1(s) &= \frac{1}{s} \left\{ c_w^2 \Sigma_T^{\gamma\gamma}(s) + 2s_w c_w \Sigma_T^{\gamma Z}(s) + s_w^2 \left[ \Sigma_T^{ZZ}(s) - \Sigma_L^{ZZ}(s) \right] \right\} \\ &= \frac{1}{2} \sum_f N_c^f \left[ \left( \frac{Y_f^L}{2c_w} \right)^2 + \left( \frac{Y_f^R}{2c_w} \right)^2 \right] \Pi_f^\gamma(s), \end{aligned} \quad (10)$$

where the vacuum-polarization function  $\Pi_f^\gamma(s)$  is defined in Eq.(61). Since  $\Pi_f^\gamma(s)$  is UV-divergent, the same must be true for  $\tilde{\Sigma}_1(s)$ . Note also that this first coefficient is proportional to  $g_1^2$ .

The mixed hypercharge–isospin coefficient  $\tilde{\Sigma}_3$  reads

$$\begin{aligned} \tilde{\Sigma}_3(s) &= \frac{1}{s} \left\{ c_w^2 \Sigma_T^{\gamma\gamma}(s) + \frac{c_w}{s_w} (s_w^2 - c_w^2) \Sigma_T^{\gamma Z}(s) - c_w^2 \left[ \Sigma_T^{ZZ}(s) - \Sigma_L^{ZZ}(s) \right] \right\} \\ &= \frac{1}{2} \frac{c_w}{s_w} \sum_f N_c^f \left( \frac{I_f^3}{s_w} \right) \left( \frac{Y_f^L}{2c_w} \right) \Pi_f^\gamma(s), \end{aligned} \quad (11)$$

which is finite because of the quantum-number identity  $\sum_f N_c^f I_f^3 Y_f^L = 0$ . With our definition, involving the extra factor  $g_1/g_2$  in Eq.(8), this coefficient is proportional to  $g_2^2$ .

The remaining two transverse, pure isospin coefficients  $\tilde{\Sigma}_2$  and  $\tilde{\Sigma}_4$  are given by

$$\tilde{\Sigma}_2(s) = \frac{1}{s} \left[ \Sigma_T^{WW}(s) - \Sigma_L^{WW}(s) \right] = \frac{1}{2} \sum_f N_c^f \left( \frac{I_f^3}{s_w} \right)^2 \Pi_f^\gamma(s) - \tilde{\Sigma}_4(s) \quad (12)$$



and

$$\begin{aligned}
\tilde{\Sigma}_4(s) &= \frac{1}{s} \left\{ s_w^2 \Sigma_T^{\gamma\gamma}(s) - 2s_w c_w \Sigma_T^{\gamma Z}(s) + c_w^2 \left[ \Sigma_T^{ZZ}(s) - \Sigma_L^{ZZ}(s) \right] \right. \\
&\quad \left. - \left[ \Sigma_T^{WW}(s) - \Sigma_L^{WW}(s) \right] \right\} \\
&= -\frac{\alpha}{24\pi s_w^2} \sum_f N_C^f \left\{ \left( 1 + \frac{2m_f^2}{s} \right) \left[ B_0(s, m_{f'}, m_f) - B_0(s, m_f, m_f) \right] \right. \\
&\quad \left. - \frac{4m_f^2(m_f^2 - m_{f'}^2)}{s^2} \left[ B_0(s, m_{f'}, m_f) - B_0(0, m_{f'}, m_f) \right] \right\}, \quad (13)
\end{aligned}$$

where the scalar two-point functions  $B_0$  are defined in the usual way [14]. The first coefficient is clearly UV-divergent and the second one clearly finite. Both coefficients are again proportional to  $g_2^2$ .

The coefficients  $\tilde{\Sigma}_3$  and  $\tilde{\Sigma}_4$  vanish at high energies ( $s \gg m_f^2$ ) and in the absence of doublet splitting ( $m_{f'} = m_f$ ). The former reflects the fact that there are only two independent self-energies in the unbroken SM, whereas the latter indicates that there is no fermion-mass-induced custodial  $SU(2)$  breaking if the fermions within an  $SU(2)$  doublet have the same mass. For  $s = 0$  we obtain  $s\tilde{\Sigma}_3(s) = s\tilde{\Sigma}_4(s) = 0$ , which implies that we can match the transverse gauge-boson sector without the explicit need for finite shifts of the gauge-boson masses. Such finite shifts will occur only in the longitudinal/scalar sector, as they should.

In the longitudinal/scalar sector we have two coefficients to match:

$$\begin{aligned}
\tilde{\Sigma}_5(s) &= -\frac{\Sigma_L^{WW}(s)}{M_w^2} \Big|_{\text{no tadpole}} = \frac{1}{8\pi^2 v^2} \sum_f N_C^f m_f^2 B_0(s, m_f, m_f) - \tilde{\Sigma}_6(s) \quad (14) \\
\tilde{\Sigma}_6(s) &= \frac{\Sigma_L^{WW}(s)}{M_w^2} - \frac{\Sigma_L^{ZZ}(s)}{M_z^2} = -\frac{1}{8\pi^2 v^2} \sum_f N_C^f m_f^2 \left\{ B_0(s, m_{f'}, m_f) \right. \\
&\quad \left. - B_0(s, m_f, m_f) - \frac{m_f^2 - m_{f'}^2}{s} \left[ B_0(s, m_{f'}, m_f) - B_0(0, m_{f'}, m_f) \right] \right\}, \quad (15)
\end{aligned}$$

where again the first coefficient is clearly UV-divergent and the second one clearly finite. As was to be expected, both coefficients are proportional to  $1/v^2$ . The finite shifts of the gauge-boson masses at  $s = 0$  have been absorbed into the

non-local  $T$ -parameter (or  $\rho$ -parameter)

$$\tilde{\Sigma}_6(0) = \frac{\Sigma_L^{WW}(0)}{M_W^2} - \frac{\Sigma_L^{ZZ}(0)}{M_Z^2} = -\frac{1}{16\pi^2 v^2} \sum_f N_c^f m_f^2 \left[ 1 - \frac{m_{f'}^2}{m_f^2 - m_{f'}^2} \log\left(\frac{m_f^2}{m_{f'}^2}\right) \right]. \quad (16)$$

Like  $\tilde{\Sigma}_3$  and  $\tilde{\Sigma}_4$ , also  $\tilde{\Sigma}_6$  vanishes at high energies ( $s \gg m_f^2$ ) and in the absence of doublet splitting ( $m_{f'} = m_f$ ).

The explicit expressions for the resummed gauge-boson propagators in the covariant  $R_\xi$  gauge can be found in Appendix A for both the transverse and longitudinal/scalar sectors.

## 2.4 Running couplings

In the sequel of this section we show explicitly how the introduction of running couplings leads to an effective description, where in analogy to the FL scheme one just has to replace bare with running couplings in tree-order matrix elements in order to properly take into account the resummed fermionic corrections. As we have seen from the explicit expressions for the various non-local coefficients, all six non-local coefficients are proportional to just one type of bare coupling. In order to make the discussion of the running couplings easier, we therefore extract these couplings from the coefficients:

$$\begin{aligned} \tilde{\Sigma}_1(s) &= g_1^2 \tilde{S}_1(s) \\ \tilde{\Sigma}_2(s) &= g_2^2 \tilde{S}_2(s) \quad , \quad \tilde{\Sigma}_3(s) = g_2^2 \tilde{S}_3(s) \quad , \quad \tilde{\Sigma}_4(s) = g_2^2 \tilde{S}_4(s) \\ \tilde{\Sigma}_5(s) &= \frac{1}{v^2} \tilde{S}_5(s) \quad , \quad \tilde{\Sigma}_6(s) = \frac{1}{v^2} \tilde{S}_6(s) \end{aligned} \quad (17)$$

with similar relations in coordinate space between  $\Sigma_i(x-y)$  and  $S_i(x-y)$  for  $i = 1, \dots, 6$ .

Upon closer investigation of Eq.(8) we notice that  $\mathcal{S}_{\text{NL}}$  contains exclusively the combinations  $\Phi/v$ ,  $g_1 B$  or  $g_2 W$ . This means that the couplings can be absorbed into the field-definition. For the corresponding local SM action we have

$$\begin{aligned} \mathcal{S}_{\text{L}} &= -\frac{1}{4g_1^2} \int d^4x g_1 B_{\mu\nu}(x) g_1 B^{\mu\nu}(x) - \frac{1}{2g_2^2} \int d^4x \text{Tr} \left[ g_2 \mathbf{F}_{\mu\nu}(x) g_2 \mathbf{F}^{\mu\nu}(x) \right] \\ &\quad + v^2 \int d^4x \frac{1}{v} \left[ D_\mu \Phi(x) \right]^\dagger \frac{1}{v} D^\mu \Phi(x) . \end{aligned} \quad (18)$$

The UV-divergences contained in the non-local coefficients  $S_i(x-y)$  have the simple form  $S_i^{\text{UV}} \delta^{(4)}(x-y)$  for  $i = 1, 2, 5$ . Combining this with the local SM

action, we end up with the minimal renormalization requirement that  $1/g_1^2 + S_1^{\text{UV}}$ ,  $1/g_2^2 + S_2^{\text{UV}}$  and  $v^2 + S_5^{\text{UV}}$  should become finite.

Having this in mind, we perform the re-diagonalization procedure in the transverse sector by introducing the running couplings

$$\begin{aligned}
\frac{1}{g_1^2(s)} &\equiv \frac{1}{s g_1^2} \left[ s + \Sigma_T^{\gamma\gamma}(s) + \frac{s_w}{c_w} \Sigma_T^{\gamma Z}(s) \right] = \frac{1}{g_1^2} + \tilde{S}_1(s) + \tilde{S}_3(s) \\
\frac{1}{g_2^2(s)} &\equiv \frac{1}{s g_2^2} \left[ s + \Sigma_T^{\gamma\gamma}(s) - \frac{c_w}{s_w} \Sigma_T^{\gamma Z}(s) \right] = \frac{1}{g_2^2} + \tilde{S}_2(s) + \tilde{S}_3(s) + \tilde{S}_4(s) \\
v^2(s) &\equiv v^2 + \tilde{S}_5(s) ,
\end{aligned} \tag{19}$$

the finiteness of which is consistent with the minimal renormalization requirement given above. From this a few more (finite) running quantities can be derived:

$$\begin{aligned}
\frac{1}{e^2(s)} &\equiv \frac{1}{4\pi\alpha(s)} \equiv \frac{1}{g_1^2(s)} + \frac{1}{g_2^2(s)} = \frac{1}{e^2} + \tilde{S}_1(s) + \tilde{S}_2(s) + 2\tilde{S}_3(s) + \tilde{S}_4(s) \\
s_w^2(s) &\equiv \frac{e^2(s)}{g_2^2(s)} \\
c_w^2(s) &\equiv 1 - s_w^2(s) = \frac{e^2(s)}{g_1^2(s)} \\
M_w^2(s) &\equiv c_w^2(s) M_Z^2(s) \equiv \frac{1}{4} v^2(s) g_2^2(s) .
\end{aligned} \tag{20}$$

At this point the correspondence with the low-energy  $S$ -,  $T$ - and  $U$ -parameters of Peskin and Takeuchi [11] can be made more explicit (see e.g. Ref. [16]):

$$\begin{aligned}
S &= 16\pi \frac{s_w^2 c_w^2}{e^2} \lim_{s \rightarrow 0} \frac{1}{s} \left\{ \Sigma_T^{ZZ}(s) - \Sigma_L^{ZZ}(s) + \frac{c_w^2 - s_w^2}{s_w c_w} \Sigma_T^{\gamma Z}(s) - \Sigma_T^{\gamma\gamma}(s) \right\} \\
&= -16\pi \tilde{S}_3(0) \\
T &= \frac{v^2}{\alpha(0) v^2(0)} \left\{ \frac{\Sigma_L^{WW}(0)}{M_W^2} - \frac{\Sigma_L^{ZZ}(0)}{M_Z^2} \right\} = \frac{1}{\alpha(0) v^2(0)} \tilde{S}_6(0) \\
U &= 16\pi \frac{s_w^2}{e^2} \lim_{s \rightarrow 0} \frac{1}{s} \left\{ \Sigma_T^{WW}(s) - \Sigma_L^{WW}(s) - c_w^2 \left[ \Sigma_T^{ZZ}(s) - \Sigma_L^{ZZ}(s) \right] \right. \\
&\quad \left. + 2s_w c_w \Sigma_T^{\gamma Z}(s) - s_w^2 \Sigma_T^{\gamma\gamma}(s) \right\} = -16\pi \tilde{S}_4(0) .
\end{aligned} \tag{21}$$

Next we want to verify that indeed all couplings have become running ones and that the propagator matrix in the transverse neutral sector has become diagonal. The easiest way to do this is by realizing that the complete matrix element for a given reaction can be written in terms of subsets of matrix elements,

each with a particular configuration of intermediate gauge bosons and associated would-be Goldstone bosons. For the discussion of a particular intermediate gauge/Goldstone boson that carries a particular momentum, the relevant set of matrix elements can be represented by a propagator function that multiplies two distinct gauge/Goldstone-boson currents. In analogy to what was done above, the trick is now to explicitly pull out the coupling strength in these currents. For the  $B$ - and  $W^a$ -currents this amounts to  $J_B = g_1 j_B$  and  $J_{W^a} = g_2 j_{W^a}$ , respectively. Similarly a factor  $1/v$  is pulled out in the would-be Goldstone-boson currents:  $J_\chi = j_\chi/v$  and  $J_\phi = j_\phi/v$ . Finally, we have to proof that the combination of propagator functions and pulled-out coupling factors gives rise to running couplings and diagonal propagators.

Let us start with the transverse neutral sector, where we have to switch to the physical mass eigenstates [see Eq.(5)]:

$$\begin{aligned} J_\gamma &= c_w J_B - s_w J_{W^3} = e (j_B - j_{W^3}) \\ J_Z &= s_w J_B + c_w J_{W^3} = s_w g_1 j_B + c_w g_2 j_{W^3} . \end{aligned} \quad (22)$$

The generic amplitude structure for intermediate transverse neutral gauge bosons then reads

$$\begin{aligned} &\begin{pmatrix} J_\gamma^\mu & J_Z^\mu \end{pmatrix} \begin{pmatrix} P_{T,\mu\nu}^{\gamma\gamma}(q) & P_{T,\mu\nu}^{\gamma Z}(q) \\ P_{T,\mu\nu}^{\gamma Z}(q) & P_{T,\mu\nu}^{ZZ}(q) \end{pmatrix} \begin{pmatrix} J_\gamma'^\nu \\ J_Z'^\nu \end{pmatrix} = \\ &\begin{pmatrix} j_B^\mu & j_{W^3}^\mu \end{pmatrix} \begin{pmatrix} e & s_w g_1 \\ -e & c_w g_2 \end{pmatrix} \begin{pmatrix} P_{T,\mu\nu}^{\gamma\gamma}(q) & P_{T,\mu\nu}^{\gamma Z}(q) \\ P_{T,\mu\nu}^{\gamma Z}(q) & P_{T,\mu\nu}^{ZZ}(q) \end{pmatrix} \begin{pmatrix} e & -e \\ s_w g_1 & c_w g_2 \end{pmatrix} \begin{pmatrix} j_B'^\nu \\ j_{W^3}'^\nu \end{pmatrix} . \end{aligned} \quad (23)$$

Using the propagator functions listed in Appendix A and the definitions of the running couplings in Eqs.(19) and (20), one can rewrite this product of matrices according to

$$\begin{aligned} &\begin{pmatrix} e & s_w g_1 \\ -e & c_w g_2 \end{pmatrix} \begin{pmatrix} P_{T,\mu\nu}^{\gamma\gamma}(q) & P_{T,\mu\nu}^{\gamma Z}(q) \\ P_{T,\mu\nu}^{\gamma Z}(q) & P_{T,\mu\nu}^{ZZ}(q) \end{pmatrix} \begin{pmatrix} e & -e \\ s_w g_1 & c_w g_2 \end{pmatrix} \\ &= \begin{pmatrix} e(s) & s_w(s) g_1(s) \\ -e(s) & c_w(s) g_2(s) \end{pmatrix} \begin{pmatrix} \bar{P}_{T,\mu\nu}^{\gamma\gamma}(q) & 0 \\ 0 & \bar{P}_{T,\mu\nu}^{ZZ}(q) \end{pmatrix} \begin{pmatrix} e(s) & -e(s) \\ s_w(s) g_1(s) & c_w(s) g_2(s) \end{pmatrix} . \end{aligned} \quad (24)$$

The diagonal transverse propagators are given by

$$\begin{aligned}
\bar{P}_{T,\mu\nu}^{\gamma\gamma}(q) &= -\frac{i}{s} \left( g_{\mu\nu} - \frac{q_\mu q_\nu}{q^2} \right) \\
\bar{P}_{T,\mu\nu}^{ZZ}(q) &= \frac{g_2^2 c_w^2(s)}{g_2^2(s) c_w^2} P_{T,\mu\nu}^{ZZ}(q) \\
&= -\frac{i}{s} \left( g_{\mu\nu} - \frac{q_\mu q_\nu}{q^2} \right) \left\{ 1 - \frac{g_2^2(s)}{c_w^2(s)} \tilde{S}_3(s) - \frac{M_Z^2(s)}{s \rho(s)} \right\}^{-1}, \quad (25)
\end{aligned}$$

using the non-local  $\rho$ -parameter

$$\rho(s) = \frac{v^2 + \tilde{S}_5(s)}{v^2 + \tilde{S}_5(s) + \tilde{S}_6(s)} = \frac{v^2(s)}{v^2(s) + \tilde{S}_6(s)}. \quad (26)$$

For the  $W$ -boson the generic amplitude structure reads

$$j_W^\mu g_2 P_{T,\mu\nu}^{WW}(q) g_2 j_W^{\prime\nu} = j_W^\mu g_2(s) \bar{P}_{T,\mu\nu}^{WW}(q) g_2(s) j_W^{\prime\nu}, \quad (27)$$

with

$$\begin{aligned}
\bar{P}_{T,\mu\nu}^{WW}(q) &= \frac{g_2^2}{g_2^2(s)} P_{T,\mu\nu}^{WW}(q) \\
&= -\frac{i}{s} \left( g_{\mu\nu} - \frac{q_\mu q_\nu}{q^2} \right) \left\{ 1 - g_2^2(s) \tilde{S}_3(s) - g_2^2(s) \tilde{S}_4(s) - \frac{M_W^2(s)}{s} \right\}^{-1}. \quad (28)
\end{aligned}$$

So, indeed all couplings have been transformed into (finite) running couplings and the effective propagators are diagonal and finite. The complex poles of the diagonalized transverse gauge-boson propagators can be obtained by solving the equations

$$\begin{aligned}
s &= 0 \\
s &= \mu_Z = \frac{M_Z^2(\mu_Z)/\rho(\mu_Z)}{1 - \frac{g_2^2(\mu_Z)}{c_w^2(\mu_Z)} \tilde{S}_3(\mu_Z)} \\
s &= \mu_W = \frac{M_W^2(\mu_W)}{1 - g_2^2(\mu_W) \tilde{S}_3(\mu_W) - g_2^2(\mu_W) \tilde{S}_4(\mu_W)}, \quad (29)
\end{aligned}$$

for the photon,  $Z$  boson and  $W$  boson, respectively.

In the longitudinal/scalar sector we get

$$\begin{aligned}
& \left( j_B^\mu \ j_{W^3}^\mu \right) \begin{pmatrix} e & s_w g_1 \\ -e & c_w g_2 \end{pmatrix} \begin{pmatrix} P_{L,\mu\nu}^{\gamma\gamma}(q, \xi_\gamma) & 0 \\ 0 & P_{L,\mu\nu}^{ZZ}(q, \xi_Z) \end{pmatrix} \begin{pmatrix} e & -e \\ s_w g_1 & c_w g_2 \end{pmatrix} \begin{pmatrix} j_B^{\prime\nu} \\ j_{W^3}^{\prime\nu} \end{pmatrix} \\
&= j_Z^\mu \frac{g_2}{2c_w} P_{L,\mu\nu}^{ZZ}(q, \xi_Z) \frac{g_2}{2c_w} j_Z^{\prime\nu} = j_Z^\mu \frac{g_2}{2c_w} \left( \frac{-i q_\mu q_\nu}{q^2} \right) D_L^{ZZ}(s, \xi_Z) \frac{g_2}{2c_w} j_Z^{\prime\nu} .
\end{aligned} \tag{30}$$

In order to achieve this simplification, the  $Z$ -boson interactions were split into an electromagnetic and isospin piece according to

$$\begin{aligned}
J_Z &= s_w g_1 j_B + c_w g_2 j_{W^3} = \frac{s_w^2 - c_w^2}{2s_w c_w} e (j_B - j_{W^3}) + \frac{g_2}{2c_w} (j_B + j_{W^3}) \\
&\equiv \frac{s_w^2 - c_w^2}{2s_w c_w} J_\gamma + \frac{g_2}{2c_w} j_Z .
\end{aligned} \tag{31}$$

The electromagnetic Ward Identity  $q \cdot J_\gamma = 0$  then takes care of all scalar electromagnetic interactions, leaving behind a pure isospin piece that has to be combined with the would-be Goldstone boson  $\chi$ . In the next step we combine the left-over  $Z$ -boson amplitude with the corresponding  $\chi$ -amplitudes:

$$\begin{aligned}
& \left( j_Z^\mu \ j_\chi \right) \begin{pmatrix} M_Z/v & 0 \\ 0 & 1/v \end{pmatrix} \begin{pmatrix} P_{L,\mu\nu}^{ZZ}(q, \xi_Z) & P_\mu^{Z\chi}(q, \xi_Z) \\ P_\nu^{XZ}(q, \xi_Z) & P^{\chi\chi}(s, \xi_Z) \end{pmatrix} \begin{pmatrix} M_Z/v & 0 \\ 0 & 1/v \end{pmatrix} \begin{pmatrix} j_Z^{\prime\nu} \\ j_\chi' \end{pmatrix} \\
&= j_\chi \frac{1}{v} \left[ -i \frac{M_Z^2}{s} D_L^{ZZ}(s, \xi_Z) - 2i M_Z P^{Z\chi}(s, \xi_Z) + P^{\chi\chi}(s, \xi_Z) \right] \frac{1}{v} j_\chi' \\
&= j_\chi \frac{1}{v(s)} \frac{i}{s} \rho(s) \frac{1}{v(s)} j_\chi' = j_\chi \frac{1}{v(s)} \frac{i}{s} \left\{ 1 + \frac{\tilde{S}_6(s)}{v^2(s)} \right\}^{-1} \frac{1}{v(s)} j_\chi' .
\end{aligned} \tag{32}$$

Here we have used the propagator functions listed in Appendix A, the running couplings as defined in Eqs.(19) and (20), and the two neutral-current Ward Identities  $q \cdot J_\gamma = 0$  and  $q \cdot J_Z = iM_Z J_\chi$  for an incoming momentum  $q$ . So, again we obtain running couplings. In a similar way we can combine the  $W$ -boson amplitudes in the longitudinal/scalar sector with the corresponding  $\phi$ -amplitudes, yielding the generic amplitude structure  $j_\phi i/[s v^2(s)] j_\phi'$ .

If we would now use the unitary gauge in the massive gauge-boson sector,  $\xi_{W/Z} \rightarrow \infty$ , all propagators involving would-be Goldstone bosons would vanish

and the dressed  $W$ -boson and  $Z$ -boson propagators would become

$$\begin{aligned}
P_{\mu\nu}^{WW}(q, \xi_W) &\xrightarrow{\xi_W \rightarrow \infty} -i \frac{g_2^2(s)}{g_2^2} \left\{ 1 - g_2^2(s) \tilde{S}_3(s) - g_2^2(s) \tilde{S}_4(s) \right\}^{-1} \frac{g_{\mu\nu} - q_\mu q_\nu / \mathcal{W}(s)}{s - \mathcal{W}(s)} \\
P_{\mu\nu}^{ZZ}(q, \xi_Z) &\xrightarrow{\xi_Z \rightarrow \infty} -i \frac{g_2^2(s) c_W^2}{g_2^2 c_W^2(s)} \left\{ 1 - \frac{g_2^2(s)}{c_W^2(s)} \tilde{S}_3(s) \right\}^{-1} \frac{g_{\mu\nu} - q_\mu q_\nu / \mathcal{Z}(s)}{s - \mathcal{Z}(s)}, \quad (33)
\end{aligned}$$

where

$$\begin{aligned}
\mathcal{W}(s) &= \frac{M_W^2(s)}{1 - g_2^2(s) \tilde{S}_3(s) - g_2^2(s) \tilde{S}_4(s)} \\
\mathcal{Z}(s) &= \frac{M_Z^2(s) / \rho(s)}{1 - \frac{g_2^2(s)}{c_W^2(s)} \tilde{S}_3(s)}. \quad (34)
\end{aligned}$$

This of course leads to a huge reduction of the effective number of Feynman rules.<sup>1</sup> These resummed expressions in the unitary gauge are a suitable starting point for the second level of matching, i.e. the renormalization, which is performed explicitly in Appendix C.

### 3 High-energy behaviour & the zero-mode solutions

Although Eq.(8) describes a gauge-invariant action, there are other properties of the local theory (SM) that are not shared by the truncated effective action. The most pronounced one is certainly unitarity and the related high-energy behaviour of the matrix elements. To exemplify this point, we have computed the matrix elements  $\mathcal{M}[e^+(p_1)e^-(p_2) \rightarrow W^+(p_+)W^-(p_-)]$  analytically. In Appendix D it is shown that the matrix element for transversely polarized  $W$  bosons and left-handed electrons exhibits an incorrect high-energy behaviour as a result of the presence of the factor

$$(p_+ p_-) \left( \frac{\tilde{\Sigma}_2(p_+^2) - \tilde{\Sigma}_2(p_-^2)}{p_+^2 - p_-^2} \right)$$

in the non-local triple gauge-boson interaction. This factor clearly diverges for large energies, unless  $\tilde{\Sigma}_2$  is a constant. Furthermore, as we will see in the next

---

<sup>1</sup>If all fermions would be massless or if there would be no doublet splitting ( $m_f = m_{f'}$ ), then  $\tilde{S}_3(s) = \tilde{S}_4(s) = \tilde{S}_6(s) = 0$  and  $\mathcal{W}(s) = M_W^2(s) = c_W^2(s) \mathcal{Z}(s)$ . In that case we reproduce the propagators of the so-called massive fermion-loop (MFL) scheme for a ‘‘massless internal world’’ [4].

section, there is a rather important numerical discrepancy in the calculation of the cross section  $\sigma(e^+e^- \rightarrow e^-\bar{\nu}_e u\bar{d})$  in the extreme forward region, which is dominated by the exchange of nearly on-shell space-like photons.

It is obvious that any difference between the BBC approach and the calculations in the FL scheme must originate from the different treatment of the three-point vertices, since the two-point functions are identical in both schemes. In order to understand the discrepancies in a more explicit way, let us define by the generic symbol  $\Delta\Gamma$  the difference between a three-point vertex as computed in the FL scheme ( $\Gamma_{\text{FL}}$ ) and the one in the BBC approach ( $\Gamma_{\text{BBC}}$ ). In the case of the photon, for instance, we obtain

$$\begin{aligned}\Delta\Gamma_{\gamma W^+ W^-}^{\mu\kappa\lambda}(q, p_+, p_-) &= \Gamma_{\text{BBC}, \gamma W^+ W^-}^{\mu\kappa\lambda} - \Gamma_{\text{FL}, \gamma W^+ W^-}^{\mu\kappa\lambda} \\ \Delta\Gamma_{\gamma W^+ \phi^-}^{\mu\kappa}(q, p_+, p_-) &= \Gamma_{\text{BBC}, \gamma W^+ \phi^-}^{\mu\kappa} - \Gamma_{\text{FL}, \gamma W^+ \phi^-}^{\mu\kappa} \\ \Delta\Gamma_{\gamma \phi^+ W^-}^{\mu\lambda}(q, p_+, p_-) &= \Gamma_{\text{BBC}, \gamma \phi^+ W^-}^{\mu\lambda} - \Gamma_{\text{FL}, \gamma \phi^+ W^-}^{\mu\lambda} \\ \Delta\Gamma_{\gamma \phi^+ \phi^-}^{\mu}(q, p_+, p_-) &= \Gamma_{\text{BBC}, \gamma \phi^+ \phi^-}^{\mu} - \Gamma_{\text{FL}, \gamma \phi^+ \phi^-}^{\mu} .\end{aligned}$$

The momenta and Lorentz indices of the incoming gauge bosons are denoted by  $(q, \mu)$  for the photon,  $(p_+, \kappa)$  for the  $W^+$  boson and  $(p_-, \lambda)$  for the  $W^-$  boson, respectively. Similarly, the momenta of the incoming would-be Goldstone bosons  $\phi^\pm$  are given by  $p_\pm$ .

Since all two-point functions are identical in the FL and BBC schemes, the above vertex quantities should satisfy a number of equations, namely Ward Identities with all two-point functions switched off. These so-called zero-mode equations can be written as

$$\begin{aligned}q_\mu \Delta\Gamma_{\gamma W^+ W^-}^{\mu\kappa\lambda}(q, p_+, p_-) &= 0 \\ p_{+\kappa} \Delta\Gamma_{\gamma W^+ W^-}^{\mu\kappa\lambda}(q, p_+, p_-) - M_W \Delta\Gamma_{\gamma \phi^+ W^-}^{\mu\lambda}(q, p_+, p_-) &= 0 \\ p_{-\lambda} \Delta\Gamma_{\gamma W^+ W^-}^{\mu\kappa\lambda}(q, p_+, p_-) + M_W \Delta\Gamma_{\gamma W^+ \phi^-}^{\mu\kappa}(q, p_+, p_-) &= 0 \\ q_\mu \Delta\Gamma_{\gamma W^+ \phi^-}^{\mu\kappa}(q, p_+, p_-) = q_\mu \Delta\Gamma_{\gamma \phi^+ W^-}^{\mu\lambda}(q, p_+, p_-) &= 0 \\ p_{+\kappa} \Delta\Gamma_{\gamma W^+ \phi^-}^{\mu\kappa}(q, p_+, p_-) - M_W \Delta\Gamma_{\gamma \phi^+ \phi^-}^{\mu}(q, p_+, p_-) &= 0 \\ p_{-\lambda} \Delta\Gamma_{\gamma \phi^+ W^-}^{\mu\lambda}(q, p_+, p_-) + M_W \Delta\Gamma_{\gamma \phi^+ \phi^-}^{\mu}(q, p_+, p_-) &= 0 \\ q_\mu \Delta\Gamma_{\gamma \phi^+ \phi^-}^{\mu}(q, p_+, p_-) &= 0 .\end{aligned}\tag{35}$$

For the  $Z$  boson one obtains a similar set of zero-mode equations. In that case, however, also the would-be Goldstone boson  $\chi$  will feature explicitly in the expressions.

In order to study the zero modes in detail, we introduce the following general



form of the triple gauge-boson vertex (excluding  $\epsilon$ -tensor contributions<sup>2</sup>):

$$\begin{aligned}
V_{\gamma W^+ W^-}^{\mu\kappa\lambda}(q, p_+, p_-) = ig_{\gamma WW} \bigg\{ & x_1 p_+^\mu g^{\kappa\lambda} + x_2 p_-^\mu g^{\kappa\lambda} + x_3 p_+^\kappa g^{\mu\lambda} + x_4 p_-^\kappa g^{\mu\lambda} \\
& + x_5 p_+^\lambda g^{\mu\kappa} + x_6 p_-^\lambda g^{\mu\kappa} + x_7 p_+^\mu p_-^\kappa p_-^\lambda + x_8 p_-^\mu p_+^\kappa p_+^\lambda \\
& + x_9 p_+^\mu p_+^\kappa p_-^\lambda + x_{10} p_-^\mu p_+^\kappa p_-^\lambda + x_{11} p_+^\mu p_-^\kappa p_+^\lambda \\
& + x_{12} p_-^\mu p_-^\kappa p_+^\lambda + x_{13} p_+^\mu p_+^\kappa p_+^\lambda + x_{14} p_-^\mu p_-^\kappa p_-^\lambda \bigg\}, \quad (36)
\end{aligned}$$

where  $g_{\gamma WW} = e$ . The coefficients  $x_i$  are scalar functions that depend on the squared momenta and masses. As a result of CP-invariance, there is a general symmetry of this vertex under the simultaneous transformations

$$p_+ \leftrightarrow -p_- \quad \text{and} \quad \kappa \leftrightarrow \lambda, \quad (37)$$

which turn incoming  $W^\pm$  bosons into outgoing  $W^\pm$  bosons with the same momenta and Lorentz indices. This results in the relation

$$x_i(q^2, p_+^2, p_-^2) \rightarrow -x_{s(i)}(q^2, p_-^2, p_+^2), \quad (38)$$

where  $s(i) = \{2, 1, 6, 5, 4, 3, 8, 7, 10, 9, 12, 11, 14, 13\}$  for  $i = \{1, \dots, 14\}$ .

A similar Lorentz-covariant parametrization can be made for the other three-point vertices:

$$\begin{aligned}
V_{\gamma W^+ \phi^-}^{\mu\kappa}(q, p_+, p_-) &= ig_{\gamma WW} \left\{ y_1 g^{\mu\kappa} + y_2 p_+^\mu p_+^\kappa + y_3 p_+^\mu p_-^\kappa + y_4 p_-^\mu p_+^\kappa + y_5 p_-^\mu p_-^\kappa \right\} \\
V_{\gamma \phi^+ W^-}^{\mu\lambda}(q, p_+, p_-) &= ig_{\gamma WW} \left\{ z_1 g^{\mu\lambda} + z_2 p_+^\mu p_+^\lambda + z_3 p_+^\mu p_-^\lambda + z_4 p_-^\mu p_+^\lambda + z_5 p_-^\mu p_-^\lambda \right\}
\end{aligned} \quad (39)$$

and

$$V_{\gamma \phi^+ \phi^-}^\mu(q, p_+, p_-) = ig_{\gamma WW} w_1 \left[ (q \cdot p_-) p_+^\mu - (q \cdot p_+) p_-^\mu \right], \quad (40)$$

where in the latter case the relevant Ward Identity has been taken into account. As a result of CP-invariance we may relate the coefficients  $y_i$  to the coefficients  $z_i$  in Eq.(39).

If we now demand that all three-point vertices satisfy Eq.(35) we end up with 25 coefficients satisfying a system of 21 equations. This can be solved algebraically in terms of 9 *coefficients*, the number of which can be reduced to 5 independent *functions* if the symmetry relations are exploited.

---

<sup>2</sup>It is well known that these terms satisfy the Ward Identities on their own, without involving the two-point functions.

In order to keep the discussion of Eq.(35) as simple as possible, we choose to neglect all contributions from vertices involving would-be Goldstone bosons by considering exclusively massless fermions. This can be done without loss of generality, since both  $\tilde{\Sigma}_2$  and the ensuing unitarity problem for transverse  $W$  bosons are also present in the unbroken theory. In that case Eq.(36) is also valid for the  $ZWW$  vertex, provided that  $g_{\gamma WW}$  is replaced by  $g_{ZWW} = -e c_w/s_w$ . It is not difficult to verify that the reduced system of zero-mode equations has always a solution and that one can express all coefficients  $x_i$  in terms of four independent ones. For instance, using  $a = p_+^2$ ,  $b = p_-^2$  and  $c = (p_+ p_-)$ , a solution may be represented by

$$\begin{aligned}
x_1 &= -\frac{b+c}{a-b} (a x_{11} + b x_{12} - a x_{13} - b x_{14}) \\
x_3 &= \frac{c(a+c)}{a-b} (x_{11} - x_{13}) + \frac{c(b+c)}{a-b} \left( x_{12} - \frac{b}{a} x_{14} \right) \\
x_4 &= \frac{a(a+c)}{a-b} (-x_{11} + x_{13}) + \frac{b+c}{a-b} (-a x_{12} + b x_{14}) \\
x_7 &= \frac{a+c}{a-b} x_{11} + \frac{b+c}{a-b} \left( x_{12} - \frac{a}{b} x_{13} - x_{14} \right) \\
x_9 &= -\frac{c}{b} x_{13} .
\end{aligned} \tag{41}$$

The rest of the coefficients are determined by using the symmetry relations (38). Notice that, although we have expressed the solution algebraically in terms of four *coefficients*, this number can be reduced to two independent *functions* by means of Eq.(38).

The four algebraically independent Lorentz structures to be used in the zero-mode solution  $\Delta \Gamma_{VW^+W^-}^{\mu\kappa\lambda}$  (for  $V = \gamma, Z$ ) may be represented as follows in momentum space. The simplest structure corresponds to  $(x_{11}, x_{12}, x_{13}, x_{14}) = (b+c, -a-c, 0, 0)$  and reads

$$V_1^{\mu\kappa\lambda} = \left[ (qp_-)p_+^\mu - (qp_+)p_-^\mu \right] \left[ (p_+p_-)g^{\kappa\lambda} - p_-^\kappa p_+^\lambda \right] . \tag{42}$$

The second one corresponds to the solution  $(1, -1, 0, 0)$ :

$$\begin{aligned}
V_2^{\mu\kappa\lambda} &= \left[ (qp_-)p_+^\mu - (qp_+)p_-^\mu \right] g^{\kappa\lambda} + g^{\mu\lambda} \left[ (p_+p_-)p_+^\kappa - p_+^2 p_-^\kappa \right] \\
&\quad - g^{\mu\kappa} \left[ (p_+p_-)p_-^\lambda - p_-^2 p_+^\lambda \right] - p_+^\mu p_-^\kappa q^\lambda + p_-^\mu q^\kappa p_+^\lambda .
\end{aligned} \tag{43}$$

Note that this vertex originates from the operator

$$\mathcal{O}_{FFF} = \text{Tr} \left[ U_2(z, x) \mathbf{F}^\mu_\nu(x) U_2(x, y) \mathbf{F}^\nu_\sigma(y) U_2(y, z) \mathbf{F}^\sigma_\mu(z) \right] ,$$

as was predicted in Eq.(1). The third structure corresponds to  $(0, 0, b, -a)$ :

$$V_3^{\mu\kappa\lambda} = \left[ p_-^2 g^{\mu\lambda} - p_-^\mu p_-^\lambda \right] \left[ (qp_+) p_+^\kappa - p_+^2 q^\kappa \right] - \left[ p_+^2 g^{\mu\kappa} - p_+^\mu p_+^\kappa \right] \left[ (qp_-) p_-^\lambda - p_-^2 q^\lambda \right]. \quad (44)$$

Finally the fourth structure corresponds to  $(0, 0, b(b+c), -a(a+c))$ :

$$V_4^{\mu\kappa\lambda} = \left[ (qp_-) p_+^\mu - (qp_+) p_-^\mu \right] \left[ p_+^2 p_-^2 g^{\kappa\lambda} - p_+^2 p_-^\kappa p_-^\lambda - p_-^2 p_+^\kappa p_+^\lambda + (p_+ p_-) p_+^\kappa p_-^\lambda \right]. \quad (45)$$

The triple gauge-boson vertex in the FL scheme, as presented in Ref. [3], can now be expressed in terms of the vertex in the BBC approach plus a linear combination of all four zero modes of Eqs.(42)–(45) [17]. It is exactly this difference between the BBC approach and the FL scheme, i.e. the zero-mode solution  $\Delta\Gamma_{VW^+W^-}^{\mu\kappa\lambda}$ , that we are after. For our purposes, however, it would be enough to just determine the zero-mode solutions that apply to either the  $q^2 \uparrow 0$  or  $q^2 \rightarrow \infty$  limits, since in those limits the BBC approach starts to deviate.

There are several ways to attack the problem, but we think that the most economical one would be to reduce as much as possible the information on the exact three-point vertex  $\Gamma_{\text{FL}, VW^+W^-}^{\mu\kappa\lambda}$ . This is motivated by the fact that we have future applications in mind where vertices with more than three gauge bosons are needed, such as six-fermion processes or four-fermion processes with an additional photon. In those cases one would like to avoid a complete fermion-loop computation as much as possible. In fact, we may further reduce the problem by taking into account the fact that, at least for four-fermion processes, we are dealing with conserved external currents. These conserved external currents are the result of either having massless fermions in the final state or having massive fermions that couple to photons. This means that terms proportional to  $q^\mu$ ,  $p_+^\kappa$  and  $p_-^\lambda$  can be neglected, leading to the following simpler form for Eq.(36):

$$V_{VW^+W^-}^{\mu\kappa\lambda}(q, p_+, p_-) = ig_{VWW} \left\{ \frac{x_1 - x_2}{2} (p_+ - p_-)^\mu g^{\kappa\lambda} + \frac{x_{11} - x_{12}}{2} (p_+ - p_-)^\mu p_-^\kappa p_+^\lambda + x_4 p_-^\kappa g^{\mu\lambda} + x_5 p_+^\lambda g^{\mu\kappa} \right\}. \quad (46)$$

The idea is now to use the information from the triple gauge-boson vertex in the FL scheme and keep only those terms that are proportional to the four tensor structures appearing in Eq.(46). The algebra of the vertex corrections has been performed with the help of Form [13], resulting in an expression in terms of tensor coefficients [14]. Subsequently, FeynCalc [15] has been used to reduce these tensor coefficients to scalar one-loop integrals according to the Passarino–Veltman decomposition. The results obtained in this way fully agree with the

ones published in Ref. [3]. In the next step, all terms proportional to the scalar three-point functions are discarded, since in the non-local approach we consider only corrections based on two-point functions. A complete set of such three-point terms obviously satisfies the zero-mode equations, but it cannot compensate any incorrect high-energy behaviour originating from the two-point sector. The remaining expressions consist of terms proportional to the scalar two-point functions  $B_0(q^2, 0, 0)$  and  $B_0(p_{\pm}^2, 0, 0)$  as well as rational terms that come from the tensor reduction and the four-dimensional limit. Since our final goal is to provide a correction term to the BBC description, it is more convenient to re-express these two-point functions in terms of the non-local coefficients  $\tilde{\Sigma}_2(q^2)$  and  $\tilde{\Sigma}_2(p_{\pm}^2)$  using the results of the previous section. Subsequently, the fermion-mass dependence is restored in  $\tilde{\Sigma}_2$ , which will allow us to take the zero-virtuality limit.

Let us first discuss the final results for the zero-mode solution in the limit  $q^2 \uparrow 0$ . These results can be represented in the following way:

$$\begin{aligned}
\delta_1 &\equiv \left(\frac{x_1 - x_2}{2}\right)_{\text{BBC}} - \left(\frac{x_1 - x_2}{2}\right)_{\text{FL}} = 0 \\
\delta_2 &\equiv \left(\frac{x_{11} - x_{12}}{2}\right)_{\text{BBC}} - \left(\frac{x_{11} - x_{12}}{2}\right)_{\text{FL}} = -16 g_{\text{BBC}} \frac{s_2 + s_3}{(s_2 - s_3)^2} - \frac{s_2 + s_3}{s_2 s_3} \tilde{\Sigma}_2(s_1) \\
&\quad + \frac{2s_2^3 - 7s_2^2 s_3 + 4s_2 s_3^2 - s_3^3}{s_2 (s_2 - s_3)^3} \tilde{\Sigma}_2(s_2) - \frac{2s_3^3 - 7s_2 s_3^2 + 4s_2^2 s_3 - s_2^3}{(s_2 - s_3)^3 s_3} \tilde{\Sigma}_2(s_3) \\
\delta_3 &\equiv (x_4)_{\text{BBC}} - (x_4)_{\text{FL}} = 16 g_{\text{BBC}} \frac{s_2}{s_2 - s_3} + \frac{s_2}{s_3} \tilde{\Sigma}_2(s_1) \\
&\quad + \frac{s_2 (-2s_2 + 3s_3)}{(s_2 - s_3)^2} \tilde{\Sigma}_2(s_2) - \frac{s_2 (s_2 - 2s_3)^2}{(s_2 - s_3)^2 s_3} \tilde{\Sigma}_2(s_3) \\
\delta_4 &\equiv (x_5)_{\text{BBC}} - (x_5)_{\text{FL}} = -\delta_3(s_2 \leftrightarrow s_3), \tag{47}
\end{aligned}$$

where we have introduced the shorthand notations  $s_1 = q^2$ ,  $s_2 = p_+^2$ ,  $s_3 = p_-^2$  as well as  $g_{\text{BBC}} = g_2^2/(64\pi^2)$ . The next step is to translate these four quantities into the basic coefficients  $x_{11}$ ,  $x_{12}$ ,  $x_{13}$  and  $x_{14}$  with the help of Eq.(41):

$$\begin{aligned}
x_{11} &= \frac{\delta_2(s_1 - s_2 + s_3) - (\delta_3 + \delta_4)}{s_1} \\
x_{13} &= \delta_1 \frac{s_2 - s_3 - s_1}{s_1 s_2} + \frac{s_3^2 - (s_2 - s_1)^2}{2s_1 s_2} \left[ \delta_2 - \frac{\delta_3 + \delta_4}{s_3 - s_2 - s_1} \right] \\
&\quad + \frac{2}{s_3 - s_2 - s_1} \left[ \delta_3 \frac{s_2 + s_3 - s_1}{2s_2} + \delta_4 \right], \tag{48}
\end{aligned}$$

with  $x_{12}$  and  $x_{14}$  determined by means of Eq.(38). These four coefficients can be inserted in Eq.(41) in order to reconstruct a complete zero-mode solution that can be subtracted safely from the BBC vertex. Note that the translation between  $\delta_1, \dots, \delta_4$  and  $x_{11}, x_{13}$ , given in Eq.(48), has by itself already an important part of the information encoded. For instance, a finite difference between the BBC and FL vertex corrections in the limit  $s_1 \uparrow 0$  is equivalent with the conditions

$$\delta_1 = 0 \quad \text{and} \quad \delta_2 = \frac{\delta_3 + \delta_4}{s_3 - s_2} ,$$

which is in full agreement with the explicit expressions in Eq.(47). These conditions guarantee that the coefficients  $x_{11}, x_{12}, x_{13}, x_{14}$  are finite, which in turn guarantees that all  $x_1, \dots, x_{14}$  are finite, since no factors  $1/s_1 = 1/(a + b + 2c)$  are present in Eq.(41).

The same exercise can be performed for the limit  $s_1 \rightarrow \infty$ . In that case we find

$$\begin{aligned} \delta_1 &= -\frac{s_1}{2} \frac{\tilde{\Sigma}_2(s_2) - \tilde{\Sigma}_2(s_3)}{s_2 - s_3} + 8 g_{\text{BBC}} - \tilde{\Sigma}_2(s_1) + \frac{s_2 \tilde{\Sigma}_2(s_2) - s_3 \tilde{\Sigma}_2(s_3)}{s_2 - s_3} \\ \delta_2 &= \frac{\tilde{\Sigma}_2(s_2) - \tilde{\Sigma}_2(s_3)}{s_2 - s_3} + \frac{2 \tilde{\Sigma}_2(s_1) - \tilde{\Sigma}_2(s_2) - \tilde{\Sigma}_2(s_3) - 16 g_{\text{BBC}}}{s_1} \\ \delta_3 &= \delta_4 = 0 , \end{aligned} \tag{49}$$

where we have kept all terms that can give rise to contributions to the amplitude that are not suppressed by inverse powers of  $s_1$ . It is not difficult to see that the leading terms in Eq.(49) can in fact be absorbed completely into the simplest zero-mode structure  $V_1$  of Eq.(42), if multiplied by

$$\frac{i g_{VWW}}{(p_+ p_-)} \left( \frac{\tilde{\Sigma}_2(s_2) - \tilde{\Sigma}_2(s_3)}{s_2 - s_3} \right) .$$

This completes the explicit construction of the zero-mode solutions that should contain the bulk of the differences between the BBC approach and the SM in the limits  $s_1 \uparrow 0$  and  $s_1 \rightarrow \infty$ . It is worthwhile to underline that the investigation performed in this section does not, by any means, address the problem of unitarization of the effective BBC action in general. The objective is to identify the differences, through the zero-mode solutions, between the BBC and the FL approach, which is manifestly unitary, in order to assess their physical significance. A numerical analysis of the importance of the zero-mode solutions is the subject of the next section.

## 4 Results

In this section we present, as an illustrative example of our approach, numerical results based on four-fermion production processes that involve interactions among three gauge bosons: the so-called CC20 and CC10 families. We focus our studies on three particular kinematical configurations:

1. the small-angle (or single- $W$ ) regime, using the process  $e^+e^- \rightarrow e^-\bar{\nu}_e u\bar{d}$  with a cut on the angle of the outgoing electron;
2. the configuration without angular cuts, using the total cross section for the process  $e^+e^- \rightarrow e^-\bar{\nu}_e u\bar{d}$  (which only involves technical cuts related to the use of massless fermions);
3. the high-energy regime, using the process  $e^+e^- \rightarrow \mu^-\bar{\nu}_\mu u\bar{d}$ .

Our numerical analysis is based on NEXTCALIBUR [18]. The matrix-element computations are performed with the help of a new version of HELAC [19] that includes all relevant vertices coming from the non-local effective action of Eq.(8), as described in Appendix A. The gauge invariance of this implementation has been checked extensively by comparing the results for the 't Hooft–Feynman and unitary gauges. Particular attention has been paid to the numerical convergence of the non-local coefficients  $\tilde{\Sigma}_i$  in all possible ranges covered by both  $q^2$  and the fermion masses. Finally, the computation of all necessary one-loop three-point tensor coefficient functions is based on the numerical programme FF [20].

The subtraction of the zero-mode solutions has been limited to the two ranges  $q^2 \uparrow 0$  and  $q^2 \rightarrow \infty$ , where  $q^2$  is the virtuality of the relevant exchanged photon or  $Z$  boson. In the former limit  $q^2 \equiv t = (p'_e - p_e)^2$ , with  $p_e$  and  $p'_e$  denoting the momenta of the incoming and the outgoing electrons. In the latter limit  $q^2 \equiv s$ , where  $s$  represents the centre-of-mass energy squared of the process.

In practice, one has to decide on the intervals of  $q^2$  in which the zero-mode corrections are switched on. In the present calculation we have selected the range  $-1 \text{ GeV}^2 \leq q^2 \leq 0$  for the first kind of zero-mode correction<sup>3</sup>. For the high-energy regime we have applied the zero-mode corrections in the full  $q^2 \geq 0$  range, since our processes are anyway dominated by double-resonant and single-resonant  $W$ -boson contributions.

In Table 1 we summarize the input parameters of our renormalization scheme and give the resulting output values for the computed quantities. Typically, three bare quantities - the electromagnetic constant  $e$ , the weak coupling  $g_2$  and the

---

<sup>3</sup>We have checked that our results remain the same when varying the lower cut-off value between  $-0.04 \text{ GeV}^2$  and  $-25 \text{ GeV}^2$ .

Higgs vacuum expectation value  $v$  - have to be fixed by three experimental data points. On the other hand, there are several well-measured experimental quantities. Therefore, in order to add part of the missing higher-order contributions and improve the predictive power of our computation, we have decided to work with five experimental data points instead of three. This means that, besides  $e$ ,  $g_2$  and  $v$ , two more parameters get fixed. The first parameter is the top-quark mass  $m_t$ , which allows an effective description of the missing non-fermionic corrections at high mass scales [2]. The second parameter is the common light-quark mass,  $m = m_u = m_d$ , which allows us to take into account the electromagnetic constant at zero virtuality. For the other fermionic masses we use their PDG values [21]. The resulting running of the renormalized electromagnetic and weak couplings are presented in Fig.1. More details on our renormalization procedure are given in Appendix C.

Input Parameters	Output values
$m_w = 80.35 \text{ GeV}$	$\sqrt{\text{Re}(\mu_w)} = 80.3235 \text{ GeV}$
$m_z = 91.1867 \text{ GeV}$	$-\frac{\text{Im}(\mu_w)}{\sqrt{\text{Re}(\mu_w)}} = 2.0575 \text{ GeV}$
$\text{Re}[\alpha^{(5)}(m_z^2)^{-1}] = 128.89$	$m_u = m_d = 0.0475188 \text{ GeV}$
$\alpha(0)^{-1} = 137.03599976$	$m_t = 146.966 \text{ GeV}$
$G_F = 1.16639 \times 10^{-5} \text{ GeV}^{-2}$	

Table 1: Input parameters versus computed quantities.

Since it is our aim to compare different schemes, we now present a few different approaches. The first one is the widely used Fixed Width (FW) scheme, where a fixed  $W$ -boson width is implemented in all  $W$ -boson propagators and where the  $G_F$ -scheme is applied for evaluating the weak parameters. We recall that the latter is defined by using  $m_w$ ,  $m_z$  and  $G_F$  as input parameters, together with the two relations

$$s_w^2 = 1 - \frac{m_w^2}{m_z^2} \quad , \quad \alpha = \frac{\sqrt{2}}{\pi} G_F m_w^2 s_w^2 .$$

In addition we introduce two hybrid schemes, where the real (imaginary) part is fixed by the FL (BBC) scheme and vice versa. This we do in order to investigate possible differences between the real and imaginary parts of the corrections that are missing in the BBC approach. Finally, we denote by BBCN the scheme that subtracts the relevant zero-mode solutions of the Ward Identities.

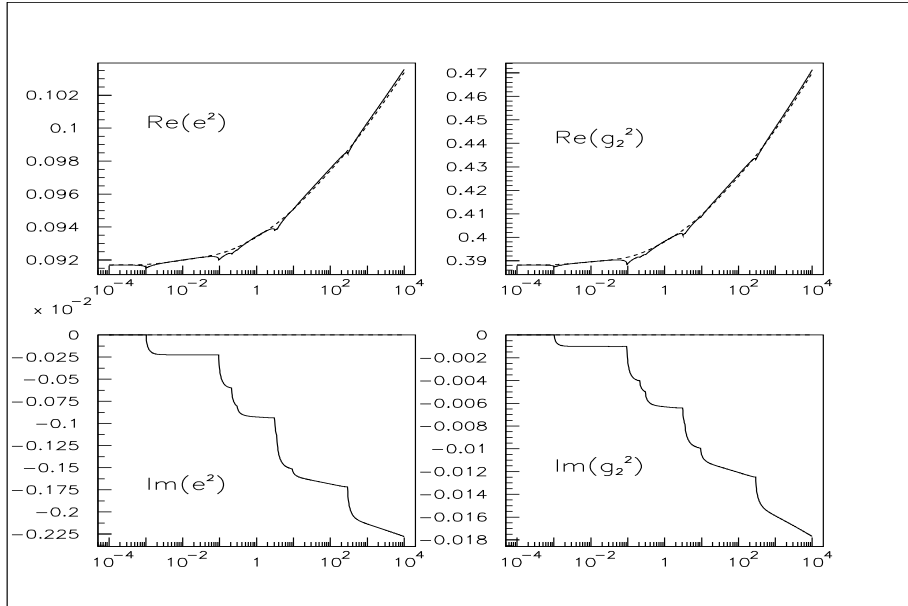


Figure 1: The evolution of the squared electromagnetic ( $e^2$ ) and weak ( $g_2^2$ ) couplings as a function of the scale  $|q|$  in GeV. The solid (dashed) line represents the evolution for positive (negative) values of  $q^2$ . The values for  $e^2$  and  $g_2^2$  predicted by the FW scheme are given by 0.09523 and 0.4260, respectively.

In order to study the small-angle behaviour of the various approximations, we focus on the reaction  $e^+e^- \rightarrow e^-\bar{\nu}_e u\bar{d}$  with the following two cuts

$$|\cos(\theta_e)| > 0.997 \quad , \quad M(u\bar{d}) > 45 \text{ GeV} .$$

The first cut, on the angle between the outgoing electron and the electron beam, ensures sensitivity to contributions that are mediated by  $t$ -channel graphs. The second cut, on the invariant mass of the  $u\bar{d}$  system, is added mainly to comply with earlier calculations. The corresponding results are presented in Table 2, from which we deduce that

- the FW scheme overestimates the cross sections by up to 6%. This is mainly due to the use of non-running couplings, especially in the electromagnetic sector;
- the BBC approach underestimates the cross sections by up to  $-6\%$ . This, in contrast to the previous case, is due to differences in the treatment of the triple gauge-boson vertex. This fact reflects the importance of subtracting zero-mode contributions;



$\sqrt{s}$ [ GeV ]	FW	BBC	Re (BBC)+Im (FL)	Re (FL)+Im (BBC)	BBCN	FL
183	89.17(26)	80.00(32)	81.80(32)	82.23(35)	84.83(32)	84.38(33) 83.28(6)
189	99.80(24)	89.38(34)	92.19(35)	92.02(35)	95.13(36)	94.60(36) 93.79(7)
200	120.98(31)	108.41(42)	111.50(43)	111.52(43)	114.69(44)	114.61(44) 113.67(8)
500	897.1(3.2)	814.8(4.6)	837.2(4.7)	833.6(5.6)	856.3(4.8)	856.3(4.8)
1000	2064(12)	1931(16)	1968(29)	2042(55)	1937(16)	1964(16)

Table 2: Cross sections (in  $fb$ ) for the process  $e^+e^- \rightarrow e^-\bar{\nu}_e u\bar{d}$ , using the cuts  $|\cos(\theta_e)| > 0.997$  and  $M(u\bar{d}) > 45$  GeV. In each second row of FL -scheme entries we give the results taken from Ref. [22], which differ slightly from our results owing to a different treatment of the hadronic part of the photonic vacuum polarization.

- the BBCN approach reproduces the results obtained in the FL scheme within MC accuracy.

In Table 3 the predicted cross section is shown for different angular regions of the outgoing electron. The four rows correspond to the FW, BBC, BBCN and FL schemes, respectively. The previous observations, which were deduced for the total cross section with angular cut  $|\cos(\theta_e)| > 0.997$ , i.e.  $\theta_e < 4.44^\circ$ , are more or less reproduced uniformly in the extreme-forward angular distribution between  $0.0^\circ$  and  $0.4^\circ$ .

In Table 4 we present results *without* angular cuts. The discrepancy is now reduced substantially, reflecting the fact that an important component of the total cross section, namely the contribution of double resonant graphs, is equally well described by the different schemes. This fact ceases to be true at energies above 500 GeV where single-resonant and multi-peripheral contributions take over again. Nevertheless the BBCN scheme still follows the FL results within MC accuracy.

Finally, as already stated, the BBC approach violates unitarity and as such gives rise to a bad high-energy behaviour. In order to better reveal this property, one has to go to rather high energies. To this end, we consider the process  $e^+e^- \rightarrow \mu^-\bar{\nu}_\mu u\bar{d}$ . The results for the corresponding total cross section are presented in Table 5, which shows rather clearly that the BBC approach and its hybrids start to diverge above 1 TeV. In contrast, the BBCN scheme exhibits a good high-energy behaviour. However, in comparison with the FW and FL schemes, the BBCN approach exhibits a substantial discrepancy above  $\sim 7$  TeV. In trying to

$\theta_e$	183 GeV	189 GeV	200 GeV
0.0° - 0.1°	49.01(17)	55.25(19)	67.81(24)
	42.98(23)	48.55(26)	59.35(32)
	46.17(24)	52.47(28)	63.73(34)
	45.56(24)	51.53(27)	63.17(34)
0.1° - 0.2°	7.03(7)	7.87(7)	9.36(9)
	6.16(9)	6.94(10)	8.35(12)
	6.77(9)	7.63(11)	8.93(13)
	6.60(9)	7.46(10)	8.84(13)
0.2° - 0.3°	4.21(5)	4.55(6)	5.40(7)
	3.59(7)	4.21(8)	4.84(9)
	3.92(7)	4.34(8)	5.17(10)
	3.87(7)	4.26(8)	5.13(10)
0.3° - 0.4°	2.80(4)	3.23(5)	3.87(6)
	2.61(6)	2.81(6)	3.55(8)
	2.85(6)	3.08(7)	3.80(8)
	2.81(6)	3.17(7)	3.76(8)

Table 3: Cross sections (in  $fb$ ) for the process  $e^+e^- \rightarrow e^-\bar{\nu}_e u\bar{d}$ , using the cut  $M(u\bar{d}) > 45$  GeV. The results are presented for different energies  $\sqrt{s}$  and for different bins of the angle  $\theta_e$  between the outgoing electron and the electron beam. The four rows correspond to the FW, BBC, BBCN and FL schemes, respectively.

$\sqrt{s}$ [GeV]	FW	BBC	Re (BBC)+Im (FL)	Re (FL)+Im (BBC)	BBCN	FL
183	766.6(1.0)	770.3(2.7)	775.3(2.7)	780.1(3.1)	773.9(2.7)	777.7(3.1)
189	808.7(1.1)	807.4(2.7)	813.3(3.0)	810.9(2.9)	815.1(2.7)	814.2(3.0)
200	851.4(1.2)	846.9(2.9)	857.1(3.0)	854.5(2.9)	859.8(3.3)	860.9(3.0)
500	1377(4)	1299(6)	1344(8)	1347(8)	1341(6)	1345(8)
1000	2555(17)	2387(16)	2463(28)	2471(30)	2414(18)	2463(27)

Table 4: Cross sections (in  $fb$ ) for the process  $e^+e^- \rightarrow e^-\bar{\nu}_e u\bar{d}$ , using only the cut  $M(u\bar{d}) > 45$  GeV, i.e. no angular cuts are imposed.

$\sqrt{s}$ [GeV]	FW	BBC	Re (BBC)+Im (FL)	Re (FL)+Im (BBC)	BBCN	FL
200	686.86(81)	702.8(2.5)	704.6(2.4)	704.6(2.4)	702.3(2.5)	704.9(2.4)
500	270.71(45)	275.5(1.2)	276.4(1.2)	276.5(1.2)	275.0(1.2)	276.3(1.2)
1000	103.67(19)	107.38(46)	106.91(47)	106.87(47)	105.84(46)	106.10(47)
2000	36.107(75)	43.36(18)	40.05(18)	40.10(19)	36.45(17)	36.89(19)
5000	8.067(25)	53.05(22)	30.35(13)	30.81(19)	8.486(61)	8.225(45)
10000	2.445(11)	187.53(62)	94.66(39)	95.31(44)	4.227(26)	2.548(27)

Table 5: Cross sections (in  $fb$ ) for the process  $e^+e^- \rightarrow \mu^-\bar{\nu}_\mu u\bar{d}$ , using the cut  $M(u\bar{d}) > 45 \text{ GeV}$ .

analyse this point, we found that the BBCN and FL schemes agree very well for massless fermions: e.g. at 10 TeV the FL scheme gives  $\sigma = 1.209(77)$  fb whereas the BBCN approach yields  $\sigma = 1.207(77)$  fb. If we would use the nominal values for the masses of the light fermions, but reduce the top-quark mass to  $m_t = 10 \text{ GeV}$ , these numbers would change to 1.226(78) and 1.233(78), respectively. Recall that in the high-energy regime the BBCN approach is defined by assuming massless fermions. The explicit fermion-mass dependence is re-introduced only through the non-local coefficients. The lesson to be learned here is that fermion masses, and more in particular the top-quark mass, play a rather important role in the triple gauge-boson vertex and cannot be accommodated by the  $\tilde{\Sigma}_2$  non-local coefficient alone.

## 5 Conclusions

In this paper we have presented an analysis that represents a first step towards an effective-action description of fermion-loop corrections to multi-fermion reactions like  $e^+e^- \rightarrow n$  fermions. The study is based on the proposal formulated in Ref. [10]. It relies on a re-organization of the expansion of the effective action of the full theory. This re-organization is performed in terms of gauge-invariant operators, involving an arbitrary number of gauge-boson and Higgs fields, multiplied by non-local coefficients. After a truncation of this expansion at the two-point-function level, a non-local effective theory is obtained that is consistent with all Ward Identities for arbitrary  $n$ -point functions.

The next important step was the identification (matching) of the non-local coefficients with the fermionic one-loop self-energy contributions predicted within the Standard Model of electroweak interactions. Applied to physical processes that do not involve interactions among more than two gauge bosons, the so-

obtained effective theory and the Standard Model lead to identical results. After renormalization, a complete description in terms of running couplings is established and the correct (fermion-loop) scale dependence is obtained, both in the high- and low-scale regimes.

Although the truncation of the expansion at the level of the two-point functions is gauge-invariant, it introduces nevertheless a bad high-energy behaviour by violating unitarity. This shows up, for instance, in the amplitudes for the production of *transversely polarized* massive gauge bosons, like  $e^+e^- \rightarrow W_T^+W_T^-$ . We have identified explicitly the zero modes of the Ward Identities that are responsible for such behaviour. Based on the appropriate high- and low-scale limits, we have reconstructed the two simplest zero-mode solutions that, if subtracted from the non-local triple gauge-boson vertex, would restore the agreement between the effective theory and the Standard Model. More specifically, we have studied the numerical effect of the zero-mode solutions for several four-fermion production processes, both for CC20 and CC10 families. We have observed the following:

- the effect of the zero modes is essential in restoring the good high-energy behaviour above  $\sim 500$  GeV;
- the zero modes also account for the substantial discrepancy between the effective theory and the Standard Model in the extreme forward region if electrons/positrons are present in the final state;
- the contribution of the zero modes to the “intermediate-energy” regime may be neglected safely.

It remains an open question how to construct in a more systematic way the relevant zero-mode solutions that will restore, to a given accuracy, the agreement between the effective theory and the Standard Model. Moreover, in order to extend the scheme to processes that involve interactions among four or more gauge bosons, like for instance six-fermion production in  $e^+e^-$  collisions, special care should be devoted to a unitarity-preserving reformulation of the non-local effective action.

## Acknowledgments

We would like to thank Frits Berends for his support during the earlier stages of this work.

## Appendix A: Non-local Feynman rules

In this appendix we list the non-local contributions to the various two-point and three-point interactions (see Ref. [10] for more details). We start off with the two-point interactions. In order to calculate the non-local propagators we add the local gauge-fixing lagrangian corresponding to the covariant  $R_\xi$  gauge:

$$\begin{aligned} \mathcal{L}_{R_\xi}(x) = & -\frac{1}{2} \left\{ \frac{1}{\xi_\gamma} \left[ \partial^\mu A_\mu(x) \right]^2 + \frac{1}{\xi_Z} \left[ \partial^\mu Z_\mu(x) - \xi_Z M_Z \chi(x) \right]^2 \right. \\ & \left. + \frac{2}{\xi_W} \left[ \partial^\mu W_\mu^+(x) - i\xi_W M_W \phi^+(x) \right] \left[ \partial^\nu W_\nu^-(x) + i\xi_W M_W \phi^-(x) \right] \right\}, \quad (50) \end{aligned}$$

where  $\xi_\gamma$ ,  $\xi_Z$  and  $\xi_W$  are gauge parameters. Taking into account all local and non-local bilinear interactions we find the following (dressed) gauge-boson propagators after inversion: ( $V = \gamma, Z, W$ )

$$\begin{aligned} P_{\mu\nu}^{VV}(q, \xi_V) &= P_{T, \mu\nu}^{VV}(q) + P_{L, \mu\nu}^{VV}(q, \xi_V) \\ &= -i D_T^{VV}(q^2) \left( g_{\mu\nu} - \frac{q_\mu q_\nu}{q^2} \right) - i D_L^{VV}(q^2, \xi_V) \frac{q_\mu q_\nu}{q^2} \\ P_{\mu\nu}^{\gamma Z}(q) &= P_{\mu\nu}^{Z\gamma}(q) = P_{T, \mu\nu}^{\gamma Z}(q) = -i D_T^{\gamma Z}(q^2) \left( g_{\mu\nu} - \frac{q_\mu q_\nu}{q^2} \right). \quad (51) \end{aligned}$$

Writing  $q^2 = s$ , the gauge-boson propagator functions  $D_T$  and  $D_L$  are given by

$$\begin{aligned} D_T^{WW}(s) &= \left\{ s \left[ 1 + \tilde{\Sigma}_2(s) \right] - M_W^2 \left[ 1 + \tilde{\Sigma}_5(s) \right] \right\}^{-1} \\ D_L^{WW}(s, \xi_W) &= \xi_W \frac{s \left[ 1 + \tilde{\Sigma}_5(s) \right] - \xi_W M_W^2}{\left[ 1 + \tilde{\Sigma}_5(s) \right] (s - \xi_W M_W^2)^2} \\ D_T^{\gamma\gamma}(s) &= s \left\{ 1 + s_w^2 \left[ \tilde{\Sigma}_1(s) - 2\tilde{\Sigma}_3(s) \right] + c_w^2 \left[ \tilde{\Sigma}_2(s) + \tilde{\Sigma}_4(s) \right] \right\} / D(s) \\ &\quad - M_Z^2 \left[ 1 + \tilde{\Sigma}_5(s) + \tilde{\Sigma}_6(s) \right] / D(s) \\ D_L^{\gamma\gamma}(s, \xi_\gamma) &= \xi_\gamma \frac{1}{s} \\ D_T^{ZZ}(s) &= s \left\{ 1 + s_w^2 \left[ \tilde{\Sigma}_2(s) + 2\tilde{\Sigma}_3(s) + \tilde{\Sigma}_4(s) \right] + c_w^2 \tilde{\Sigma}_1(s) \right\} / D(s) \end{aligned}$$

$$\begin{aligned}
D_L^{ZZ}(s, \xi_Z) &= \xi_Z \frac{s \left[ 1 + \tilde{\Sigma}_5(s) + \tilde{\Sigma}_6(s) \right] - \xi_Z M_Z^2}{\left[ 1 + \tilde{\Sigma}_5(s) + \tilde{\Sigma}_6(s) \right] (s - \xi_Z M_Z^2)^2} \\
D_T^{\gamma Z}(s) &= -s s_w c_w \left[ \tilde{\Sigma}_1(s) - \tilde{\Sigma}_2(s) - \tilde{\Sigma}_3(s) - \tilde{\Sigma}_4(s) + \frac{s_w^2}{c_w^2} \tilde{\Sigma}_3(s) \right] / D(s) ,
\end{aligned} \tag{52}$$

with

$$\begin{aligned}
D(s) &= s^2 \left\{ \left[ 1 + \tilde{\Sigma}_1(s) \right] \left[ 1 + \tilde{\Sigma}_2(s) + \tilde{\Sigma}_4(s) \right] - \frac{s_w^2}{c_w^2} \left[ \tilde{\Sigma}_3(s) \right]^2 \right\} \\
&\quad - s M_Z^2 \left[ 1 + \tilde{\Sigma}_5(s) + \tilde{\Sigma}_6(s) \right] \left\{ 1 + s_w^2 \left[ \tilde{\Sigma}_2(s) + 2\tilde{\Sigma}_3(s) + \tilde{\Sigma}_4(s) \right] + c_w^2 \tilde{\Sigma}_1(s) \right\} .
\end{aligned} \tag{53}$$

Note that  $D_T^{WW}(0) = D_L^{WW}(0)$  and  $D_T^{ZZ}(0) = D_L^{ZZ}(0)$  as a result of analyticity requirements.

The dressed propagators involving the would-be Goldstone bosons are relatively simple:

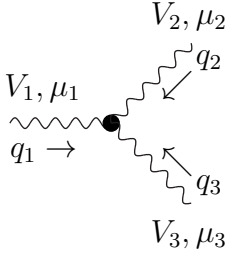
$$\begin{aligned}
P_\mu^{W^\pm \phi^\mp}(q, \xi_w) &= P_\mu^{\phi^\pm W^\mp}(q, \xi_w) = \pm i q_\mu \frac{\xi_w M_w \tilde{\Sigma}_5(s)}{\left[ 1 + \tilde{\Sigma}_5(s) \right] (s - \xi_w M_w^2)^2} \\
&\equiv q_\mu P^{W^\pm \phi^\mp}(s, \xi_w) \\
P^{\phi\phi}(s, \xi_w) &= i \frac{s - \xi_w M_w^2 \left[ 1 + \tilde{\Sigma}_5(s) \right]}{\left[ 1 + \tilde{\Sigma}_5(s) \right] (s - \xi_w M_w^2)^2} \\
P_\mu^{Z\chi}(q, \xi_Z) &= -P_\mu^{\chi Z}(q, \xi_Z) = -q_\mu \frac{\xi_Z M_Z \left[ \tilde{\Sigma}_5(s) + \tilde{\Sigma}_6(s) \right]}{\left[ 1 + \tilde{\Sigma}_5(s) + \tilde{\Sigma}_6(s) \right] (s - \xi_Z M_Z^2)^2} \\
&\equiv q_\mu P^{Z\chi}(s, \xi_Z) \\
P^{\chi\chi}(s, \xi_Z) &= i \frac{s - \xi_Z M_Z^2 \left[ 1 + \tilde{\Sigma}_5(s) + \tilde{\Sigma}_6(s) \right]}{\left[ 1 + \tilde{\Sigma}_5(s) + \tilde{\Sigma}_6(s) \right] (s - \xi_Z M_Z^2)^2} .
\end{aligned} \tag{54}$$

Now we come to the three-point vertices. For a compact notation we first

introduce the following three tensor structures:

$$\begin{aligned}
T^{\mu_1\mu_2}(q_1, q_2) &= (q_1q_2)g^{\mu_1\mu_2} - q_1^{\mu_2}q_2^{\mu_1} \\
A^{\mu_1, \mu_2\mu_3}(q) &= g^{\mu_1\mu_2}q^{\mu_3} - g^{\mu_1\mu_3}q^{\mu_2} \\
\mathcal{A}_5^\mu(q_1, q_2) &= \frac{\tilde{\Sigma}_5(q_2^2) - \tilde{\Sigma}_5(q_1^2)}{q_2^2 - q_1^2} (q_2 - q_1)^\mu .
\end{aligned} \tag{55}$$

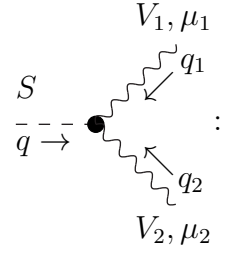
In terms of these tensor structures the non-local three-point interactions read



$$\begin{aligned}
& : ig_2 \left\{ A_2 \sum_{\text{perm}} \epsilon^{jkl} \tilde{\Sigma}_2(q_j^2) \left[ \frac{(2q_j + q_l)^{\mu_l}}{(q_j + q_l)^2 - q_j^2} T^{\mu_j\mu_k}(q_j, q_k) \right. \right. \\
& \quad \left. \left. + \frac{1}{2} A^{\mu_j, \mu_k\mu_l}(q_j) \right] + A^{\mu_1, \mu_2\mu_3}(q_1) \left[ A_{31} \tilde{\Sigma}_3(q_1^2) + A_{41} \tilde{\Sigma}_4(q_1^2) \right] \right. \\
& \quad \left. + \frac{M_W^2}{2c_W} \sum_{\text{perm}} A_{jkl} g^{\mu_j\mu_k} \mathcal{A}_5^{\mu_l}(q_j, q_k) \right\} .
\end{aligned} \tag{56}$$

The summation includes all possible permutations  $(j, k, l)$  of  $(1, 2, 3)$  and the various couplings are given by

$V_1V_2V_3$	$A_2$	$A_{31}$	$A_{41}$	non-zero coefficients $A_{jkl}$
$\gamma W^+W^-$	$s_W$	$s_W$	$s_W$	$A_{231} = 2c_W s_W$
$ZW^+W^-$	$-c_W$	$s_W^2/c_W$	$-c_W$	$A_{123} = -A_{132} = -1$ , $A_{231} = s_W^2 - c_W^2$

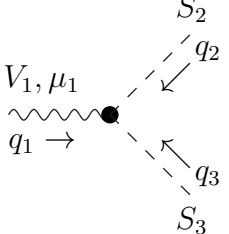


$$\begin{aligned}
& : \frac{ig_2}{M_W} \left\{ T^{\mu_1\mu_2}(q_1, q_2) \left[ \frac{s_W}{c_W} \left[ C_{31} \tilde{\Sigma}_3(q_1^2) + C_{32} \tilde{\Sigma}_3(q_2^2) \right] + C_{41} \tilde{\Sigma}_4(q_1^2) \right. \right. \\
& \quad \left. \left. + C_{42} \tilde{\Sigma}_4(q_2^2) \right] - \frac{M_W^2}{2c_W} \sum_{\text{perm}} \left[ C_{5jk} \left[ q^{\mu_j} \mathcal{A}_5^{\mu_k}(q_j, q) \right. \right. \right. \\
& \quad \left. \left. \left. + g^{\mu_j\mu_k} \tilde{\Sigma}_5(q_j^2) \right] + 2g^{\mu_j\mu_k} C_{6jk} \tilde{\Sigma}_6(q_j^2) \right] \right\} .
\end{aligned} \tag{57}$$

The summation includes all possible permutations  $(j, k)$  of  $(1, 2)$  and the various

couplings are given by

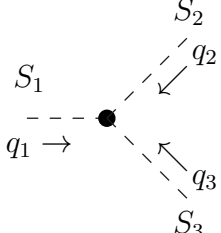
$SV_1V_2$	$C_{31}$	$C_{32}$	$C_{41}$	$C_{42}$	$C_{512}$	$C_{521}$	$C_{612}$	$C_{621}$
$HZZ$	$-s_w c_w$	$-s_w c_w$	$c_w^2$	$c_w^2$	$-1/c_w$	$-1/c_w$	$-1/c_w$	$-1/c_w$
$HZ\gamma$	$s_w^2$	$-c_w^2$	$-s_w c_w$	$-s_w c_w$	0	0	0	0
$H\gamma\gamma$	$s_w c_w$	$s_w c_w$	$s_w^2$	$s_w^2$	0	0	0	0
$HW^+W^-$	0	0	0	0	$-c_w$	$-c_w$	0	0
$\chi W^+W^-$	0	0	0	0	$i c_w$	$-i c_w$	0	0
$\phi^\mp ZW^\pm$	$s_w$	0	$-c_w$	0	1	$s_w^2 - c_w^2$	1	0
$\phi^\mp \gamma W^\pm$	$c_w$	0	$s_w$	0	0	$2s_w c_w$	0	0



$$: -\frac{ie}{2c_w s_w} \left\{ E_1 \left[ (q_2 q_3) \mathcal{A}_5^{\mu_1}(q_2, q_3) + q_2^{\mu_1} \tilde{\Sigma}_5(q_2^2) - q_3^{\mu_1} \tilde{\Sigma}_5(q_3^2) \right] + E_{23} (q_2 - q_3)^{\mu_1} \tilde{\Sigma}_6(q_1^2) + E_3 q_3^{\mu_1} \tilde{\Sigma}_6(q_3^2) \right\}. \quad (58)$$

The various couplings are given by

$V_1 S_2 S_3$	$E_1$	$E_{23}$	$E_3$
$Z\phi^+\phi^-$	$s_w^2 - c_w^2$	1	0
$\gamma\phi^+\phi^-$	$2c_w s_w$	0	0
$ZH\chi$	$-i$	$-i$	$2i$
$W^\pm H\phi^\mp$	$\mp c_w$	0	0
$W^\pm \phi^\mp \chi$	$i c_w$	0	$-2i c_w$



$$: -\frac{i}{v} \sum_{\text{perm}} (q_j q_l) F_{jkl} \tilde{\Sigma}_6(q_j^2). \quad (59)$$

The summation includes all possible permutations  $(j, k, l)$  of  $(1, 2, 3)$  and the various couplings are given by

$S_1 S_2 S_3$	non-zero coefficients $F_{jkl}$
$HHH$	$F_{jkl} = 1$ for all permutations of $(1, 2, 3)$
$H\chi\chi$	$F_{123} = F_{132} = -F_{231} = -F_{321} = F_{213} = F_{312} = 1$
$H\phi^+\phi^-$	$F_{123} = F_{132} = 1$
$\chi\phi^+\phi^-$	$F_{123} = -F_{132} = i$



## Appendix B: Two-point functions in the FL scheme

In this appendix we list the various unrenormalized fermion-loop self-energies in the SM, which will be needed for determining the six non-local coefficients.

The gauge-boson self-energies can be written as:

$$\begin{array}{c} V_1, \mu \\ \text{~~~~~} \circlearrowleft \text{~~~~~} \\ q \rightarrow \quad \leftarrow -q \\ \text{~~~~~} V_2, \nu \end{array} : i \Sigma_{\mu\nu}^{V_1 V_2}(q) = -i \Sigma_T^{V_1 V_2}(q^2) \left( g_{\mu\nu} - \frac{q_\mu q_\nu}{q^2} \right) - i \Sigma_L^{V_1 V_2}(q^2) \frac{q_\mu q_\nu}{q^2}, \quad (60)$$

where  $\Sigma_T$  and  $\Sigma_L$  are the transverse and longitudinal gauge-boson self-energies, respectively. Writing  $q^2 = s$ , we find for the transverse self-energies

$$\begin{aligned} \Sigma_T^{\gamma\gamma}(s) &= \frac{\alpha}{3\pi} \sum_f N_C^f Q_f^2 \left\{ s \left[ B_0(s, 0, 0) - \frac{1}{3} \right] + s \left[ B_0(s, m_f, m_f) - B_0(s, 0, 0) \right] \right. \\ &\quad \left. + 2m_f^2 \left[ B_0(s, m_f, m_f) - B_0(0, m_f, m_f) \right] \right\} \equiv s \sum_f N_C^f Q_f^2 \Pi_f^\gamma(s) \quad (61) \end{aligned}$$

and

$$\begin{aligned} \Sigma_T^{\gamma Z}(s) &= -s \sum_f N_C^f \left[ \frac{|Q_f|}{4s_w c_w} - \frac{s_w}{c_w} Q_f^2 \right] \Pi_f^\gamma(s) \\ \Sigma_T^{ZZ}(s) &= s \sum_f N_C^f \left[ \frac{(c_w^2 - s_w^2)|Q_f|}{4s_w^2 c_w^2} + \frac{s_w^2}{c_w^2} Q_f^2 \right] \Pi_f^\gamma(s) + \frac{T_Z(s)}{c_w^2} \\ \Sigma_T^{WW}(s) &= s \sum_f N_C^f \frac{|Q_f|}{4s_w^2} \Pi_f^\gamma(s) + T_w(s). \quad (62) \end{aligned}$$

The scalar two-point functions  $B_0$  are defined in the usual way [14] and

$$\begin{aligned} T_Z(s) &= 2M_w^2 T - \frac{\alpha}{8\pi s_w^2} \sum_f N_C^f m_f^2 B_0(s, m_f, m_f) - s \sum_f N_C^f \frac{2|Q_f| - 1}{8s_w^2} \Pi_f^\gamma(s) \\ T_w(s) &= T_Z(s) + \frac{\alpha}{24\pi s_w^2} \sum_f N_C^f \left\{ (s - m_f^2) \left[ B_0(s, m_{f'}, m_f) - B_0(s, m_f, m_f) \right] \right. \\ &\quad \left. - \frac{m_f^2(m_f^2 - m_{f'}^2)}{s} \left[ B_0(s, m_{f'}, m_f) - B_0(0, m_{f'}, m_f) \right] \right\}. \quad (63) \end{aligned}$$



boson:

$$\begin{aligned} \Sigma^{HH}(s) = & 3M_H^2 T - \frac{1}{8\pi^2 v^2} \sum_f N_C^f m_f^2 \left\{ (4m_f^2 - s)B_0(s, m_f, m_f) \right. \\ & \left. + 2m_f^2 [B_0(0, m_f, m_f) + 1] \right\}. \end{aligned} \quad (68)$$

The above-given longitudinal/scalar self-energies satisfy the following Ward Identities:

$$\Sigma_L^{ZZ}(s) - 2iM_Z \Sigma^{Z\chi}(s) - \frac{M_Z^2}{s} \Sigma^{\chi\chi}(s) = 0 \quad (69)$$

$$\Sigma_L^{WW}(s) \pm 2M_W \Sigma^{W\pm\phi^\mp}(s) - \frac{M_W^2}{s} \Sigma^{\phi\phi}(s) = 0. \quad (70)$$

As a next step we perform tadpole renormalization. This involves shifting the bare vacuum in such a way that at one-loop level it coincides with the true vacuum of the Higgs potential. Or in other words, the one-point counterterm generated by the finite shift of the bare vacuum  $v$  completely compensates the tadpole self-energy terms  $\propto T$ . This is equivalent to the following effective procedure: keep the bare vacuum as it is, but remove the terms  $\propto T$  from the  $WW$ ,  $ZZ$ ,  $W\phi$ ,  $Z\chi$ , and  $HH$  self-energies. The  $\phi\phi$  and  $\chi\chi$  self-energies receive both one-point and two-point counterterms, which exactly cancel each other. So, the tadpole contributions to these self-energies should be kept and are therefore merged with the rest of the fermion-loop corrections. This is a trivial exercise, since the  $\phi\phi$  and  $\chi\chi$  self-energies have an internal cancellation of all terms  $\propto T$  (see the expressions above).

## Appendix C: Renormalization conditions

An essential ingredient of the matching procedure is the renormalization of the non-local coefficients, which takes the form of matching the non-local matrix elements and cross sections with explicit experimental observables. Various options are open, each with their own merits. Let us go through the most popular renormalization/matching conditions, bearing in mind that we only have to fix the running couplings  $v^2(s)$ ,  $1/g_2^2(s)$  and  $1/e^2(s)$ .

**Muon decay:** One of the often applied matching conditions is based on the charged-current muon-decay process  $\mu^- \rightarrow \nu_\mu e^- \bar{\nu}_e$ . In the unitary gauge we

obtain the matrix element

$$\mathcal{M}_1 = -\frac{g_2^2}{2} P_{\rho\sigma}^{WW}(q_W, \xi_W \rightarrow \infty) [\bar{u}_{\nu_\mu}(p_{\nu_\mu}) \gamma^\rho \omega_- u_\mu(p_\mu)] [\bar{u}_e(p_e) \gamma^\sigma \omega_- v_{\nu_e}(p_{\bar{\nu}_e})], \quad (71)$$

with  $q_W = p_e + p_{\bar{\nu}_e}$  and  $\omega_\pm = (1 \pm \gamma_5)/2$ . Upon neglecting  $m_e$  and  $m_\mu$  with respect to  $M_W$ , the expression simplifies to

$$\mathcal{M}_1 = \frac{i}{\mathcal{V}_1(q_W^2)} [\bar{u}_{\nu_\mu}(p_{\nu_\mu}) \gamma^\rho \omega_- u_\mu(p_\mu)] [\bar{u}_e(p_e) \gamma_\rho \omega_- v_{\nu_e}(p_{\bar{\nu}_e})] \quad (72)$$

in terms of the inverse amplitude

$$\mathcal{V}_1(q_W^2) = 2q_W^2 \left[ \frac{1}{g_2^2(q_W^2)} - \tilde{S}_3(q_W^2) - \tilde{S}_4(q_W^2) \right] - \frac{1}{2} v^2(q_W^2). \quad (73)$$

This final step was obtained with the help of Eqs.(20), (33) and (34). In the muon-decay process we can go one step further, since  $q_W^2 = \mathcal{O}(m_\mu^2) \ll M_W^2$ . In that case the (low-energy) inverse amplitude reads  $\mathcal{V}_1(0) = -v^2(0)/2$ . The actual matching condition links this inverse amplitude to the experimentally-determined coefficient of the effective (low-energy) charged-current  $V-A$  lagrangian

$$\mathcal{L}_{\text{eff}} = -2\sqrt{2} G_F [\bar{\psi}_{\nu_\mu} \gamma^\rho \omega_- \psi_\mu] [\bar{\psi}_e \gamma_\rho \omega_- \psi_{\nu_e}] + \dots \quad (74)$$

In this way we obtain

$$v^2(0) = v^2 + \tilde{S}_5(0) = \frac{1}{\sqrt{2} G_F} \Rightarrow v^2(s) = \frac{1}{\sqrt{2} G_F} + \tilde{S}_5(s) - \tilde{S}_5(0). \quad (75)$$

**The  $W$ -boson mass:** A second, optional matching condition involves the mass of the  $W$  bosons. For the definition we can again make use of the inverse amplitude  $\mathcal{V}_1(q_W^2)$ . The most commonly used procedure is the on-shell condition

$$\text{Re} \left[ \mathcal{V}_1(m_W^2) \right] = 0 \Rightarrow \frac{1}{g_2^2} = \frac{\text{Re } v^2(m_W^2)}{4m_W^2} - \text{Re } \tilde{S}_2(m_W^2), \quad (76)$$

where  $m_W$  is the experimentally-determined  $W$ -boson mass (based on an on-shell analysis). This results in

$$\frac{1}{g_2^2(s)} = \frac{\text{Re } v^2(m_W^2)}{4m_W^2} - \text{Re } \tilde{S}_2(m_W^2) + \tilde{S}_2(s) + \tilde{S}_3(s) + \tilde{S}_4(s). \quad (77)$$

The on-shell procedure breaks down if one includes two-loop corrections [23], therefore it is sometimes better to use the complex  $W$ -boson pole  $\mu_W$  in the matching procedure:

$$\mathcal{V}_1(\mu_W) = 0 \Rightarrow \frac{1}{g_2^2} = \frac{v^2(\mu_W)}{4\mu_W} - \tilde{S}_2(\mu_W). \quad (78)$$

The real part of this complex pole can now be identified with the experimentally-determined  $W$ -boson mass, provided the same complex procedure is adopted in the data analysis.

**The  $Z$ -boson mass:** A very precisely known experimental observable is the  $Z$ -boson mass, so it is a natural candidate for performing the matching. A defining process for the  $Z$ -boson mass is the reaction  $\nu_e \bar{\nu}_e \rightarrow \nu_\mu \bar{\nu}_\mu$ , which leads in the unitary gauge to the following (inverse) amplitude:

$$\begin{aligned} \mathcal{M}_2 &= \frac{i}{\mathcal{V}_2(q_Z^2)} [\bar{u}_{\nu_\mu}(p_{\nu_\mu}) \gamma^\rho \omega_- v_{\nu_\mu}(p_{\bar{\nu}_\mu})] [\bar{v}_{\nu_e}(p_{\bar{\nu}_e}) \gamma_\rho \omega_- u_{\nu_e}(p_{\nu_e})] \\ \mathcal{V}_2(q_Z^2) &= 4q_Z^2 \left[ \frac{c_W^2(q_Z^2)}{g_2^2(q_Z^2)} - \tilde{S}_3(q_Z^2) \right] - v^2(q_Z^2) - \tilde{S}_6(q_Z^2), \end{aligned} \quad (79)$$

with  $q_Z = p_{\nu_e} + p_{\bar{\nu}_e}$ . This expression was again obtained with the help of Eqs.(20), (33) and (34). Using Eqs.(19) and (20), the experimentally-determined value of the  $Z$ -boson mass in the on-shell approach ( $m_Z$ ) and the on-shell condition  $\text{Re } \mathcal{V}_2(m_Z^2) = 0$ , one arrives at the following quadratic equation:

$$\begin{aligned} 0 &= \frac{\text{Re } A}{g_2^4} + \frac{\text{Re } B}{g_2^2} + \text{Re } C \\ A &= e^2(m_Z^2) \\ B &= 2e^2(m_Z^2) \left[ \tilde{S}_2(m_Z^2) + \tilde{S}_3(m_Z^2) + \tilde{S}_4(m_Z^2) \right] - 1 \\ C &= \frac{v^2(m_Z^2) + \tilde{S}_6(m_Z^2)}{4m_Z^2} + e^2(m_Z^2) \left[ \tilde{S}_2(m_Z^2) + \tilde{S}_3(m_Z^2) + \tilde{S}_4(m_Z^2) \right]^2 \\ &\quad - \tilde{S}_2(m_Z^2) - \tilde{S}_4(m_Z^2). \end{aligned} \quad (80)$$

The relevant solution is given by

$$\frac{1}{g_2^2} = \frac{1}{2 \text{Re } A} \left\{ -\text{Re } B - \sqrt{(\text{Re } B)^2 - 4 \text{Re } A \text{Re } C} \right\}. \quad (81)$$

For a matching procedure based on the complex  $Z$ -boson pole,  $\mu_Z$ , one merely has to replace  $\text{Re } A$ ,  $\text{Re } B$ ,  $\text{Re } C$  and  $m_Z^2$  by  $A$ ,  $B$ ,  $C$  and  $\mu_Z$ .

**The electromagnetic coupling:** The matching condition for the electromagnetic coupling has to be addressed with care, in view of its far-reaching consequences for the low- and high-scale behaviour of the cross sections. The complication is caused by the hadronic part of the photonic vacuum polarization, which

is sensitive to non-perturbative strong-interaction effects through the exchange of gluons with low momentum transfer.

We can either match at a high scale, like  $q_\gamma^2 = m_z^2$ , or at a low scale, like the Thomson limit  $q_\gamma^2 = 0$ . In the former case we have to evolve the running coupling down to low scales in order to deal with phenomena that involve nearly on-shell photons (cf. single  $W$  production). In the latter case we have to evolve the running coupling up to high scales in order to properly describe high-scale reactions. From this it should be clear that preferably we want to match the complete running of the electromagnetic coupling, instead of matching it in a single point. To this end we have to exploit the explicit parametric dependence of the non-local coefficients, i.e. the dependence on the fermion masses  $m_f$ . It has no use fiddling around with the lepton masses, since these masses are experimentally well-known and the leptonic evolution of the electromagnetic coupling is free of ambiguities. The same does not apply to the hadronic part of the photonic vacuum polarization, in view of the various light-quark bound states that contribute. So, the light-quark masses are prime candidates for tuning the evolution of the electromagnetic coupling.

We start with the electromagnetic coupling at the LEP1  $Z$  peak. Usually this coupling is presented for five active quark flavours and without imaginary part, i.e.  $\text{Re}[\alpha^{(5)}(m_z^2)^{-1}]$ . The relation between  $\alpha^{(5)}(s)$  and  $\alpha(s)$  is fixed by the requirement of top-quark decoupling at  $s = 0$ :

$$\frac{1}{\alpha(s)} = \frac{1}{\alpha} + \sum_f N_c^f Q_f^2 \frac{\Pi_f^\gamma(s)}{\alpha} = \frac{1}{\alpha^{(5)}(s)} + N_c^t Q_t^2 \frac{\Pi_t^\gamma(s) - \Pi_t^\gamma(0)}{\alpha} . \quad (82)$$

By fixing the value of  $\text{Re}[\alpha^{(5)}(m_z^2)^{-1}] \equiv \alpha_z^{-1}$  we obtain

$$\frac{1}{e^2} = \frac{1}{4\pi\alpha} = \frac{1}{4\pi\alpha_z} - \sum_{f \neq t} N_c^f Q_f^2 \text{Re} \left[ \frac{\Pi_f^\gamma(m_z^2)}{e^2} \right] - N_c^t Q_t^2 \frac{\Pi_t^\gamma(0)}{e^2} . \quad (83)$$

The leptonic as well as top-quark contributions can now be calculated perturbatively. Subsequently we tune the evolution to lower scales by using a set of effective light-quark masses. In the standard procedure this set of light-quark masses represents a perturbative fit to the once-subtracted dispersion integral of the experimental observable  $R^\gamma(s) = \frac{3s}{4\pi\alpha^2(0)} \sigma(e^+e^- \rightarrow \gamma^* \rightarrow \text{hadrons})$ :

$$\sum_{f=q, f \neq t} N_c^f Q_f^2 \frac{\Pi_f^\gamma(s) - \Pi_f^\gamma(0)}{4\pi\alpha} = \frac{s}{12\pi^2} \int_{4m_\pi^2}^{\infty} ds' \frac{R^\gamma(s')}{s'(s' - s - i\varepsilon)} , \quad (84)$$

which automatically covers all non-perturbative hadronic contributions. Note that in this way the quality of  $\alpha(0)$  is linked to the quality of the effective-mass parametrization at the matching scale  $s = m_Z^2$  and to the quality of the perturbative calculation used in the fit. This can be circumvented by adopting an alternative procedure, which uses the value of  $\alpha(0) \equiv \alpha_0$  as additional matching condition, leading to

$$\frac{1}{e^2} = \frac{1}{4\pi\alpha_0} - \sum_f N_c^f Q_f^2 \frac{\Pi_f^\gamma(0)}{e^2}. \quad (85)$$

This second matching condition can be implemented by tuning the effective  $u$ - and  $d$ -quark masses.

Based on the matching conditions discussed above, various matching procedures are possible.

**1) The LEP1 procedure** : this procedure combines the measured top-quark mass at the Tevatron with three of the above-mentioned matching conditions, i.e. the muon-decay condition and the two on-shell LEP1 conditions for the  $Z$ -boson mass and the electromagnetic coupling. So, with this procedure the input parameters are  $G_F$ ,  $m_Z$ ,  $\text{Re}[\alpha^{(5)}(m_Z^2)^{-1}] \equiv \alpha_Z^{-1}$ ,  $m_t$ , the lepton masses and the standard set of effective light-quark masses.

**2) The LEP2 procedure** : this procedure adds the on-shell  $W$ -boson mass  $m_W$  to the matching conditions of the LEP1 procedure. Because  $1/g_2^2$  is now matched twice, we end up with a consistency relation. The dominant ingredient in this relation is the top-quark contribution. Therefore we can determine the top-quark mass by solving the consistency relation iteratively. Since we exclusively take into account fermion loops, the resulting top-quark mass will be an effective parameter that mimics bosonic loop effects. Its value will come out appreciably lower than the experimental measurement (see Ref. [3]).

**3) Our procedure** : in the present analysis we have added the electromagnetic coupling in the Thomson limit,  $\alpha(0) \equiv \alpha_0$ , to the matching conditions of the LEP2 procedure. This results in an alternative set of effective light-quark masses, with adjusted values for the  $u$ - and  $d$ -quark masses. Moreover, we have replaced the on-shell conditions for the  $W$ - and  $Z$ -boson masses by their complex counterparts. So, we use Eqs.(75), (78), (83) and (85), as well as the complex version of Eq.(81). This system of equations is solved iteratively, resulting in the determination of

the complex gauge-boson poles  $\mu_{W,Z}$ , the effective top-quark mass  $m_t$  and the effective common light-quark mass  $m_u = m_d$ .

## Appendix D: $e^+e^- \rightarrow W_T^+W_T^-$ and high-energy unitarity

In this appendix we have a closer look at the process of on-shell transverse  $W$ -pair production,  $e^+(p_1)e^-(p_2) \rightarrow W_T^+(p_+)W_T^-(p_-)$ , in the high-energy limit. Neglecting the electron mass, the momenta of the particles are defined as follows in the initial-state centre-of-mass frame:

$$\begin{aligned} p_1 &= \frac{\sqrt{s}}{2} (1, 0, 0, 1), & p_+ &= \frac{\sqrt{s}}{2} (1, 0, \beta \sin \theta, \beta \cos \theta) \\ p_2 &= \frac{\sqrt{s}}{2} (1, 0, 0, -1), & p_- &= \frac{\sqrt{s}}{2} (1, 0, -\beta \sin \theta, -\beta \cos \theta), \end{aligned}$$

where  $\theta$  is the scattering angle and  $\beta = \sqrt{1 - 4M_W^2/s}$  is the velocity of the  $W$  bosons. In this frame the polarization vectors for transversely polarized  $W$  bosons are given by

$$\begin{aligned} \epsilon_{\pm}^{\mu}(p_+) &= \frac{1}{\sqrt{2}} (0, i, \mp \cos \theta, \pm \sin \theta) \\ \epsilon_{\pm}^{\mu}(p_-) &= \frac{1}{\sqrt{2}} (0, -i, \mp \cos \theta, \pm \sin \theta), \end{aligned}$$

where the subscripts  $\pm$  indicate the transverse helicities  $\pm 1$  of the considered  $W$  boson. Note that these polarization vectors are orthogonal with respect to both  $p_+$  and  $p_-$ . Finally, the left- and right-handed electron-positron currents can be written as

$$\begin{aligned} J_L^{\mu} &= \bar{v}_e(p_1)\gamma^{\mu}\omega_-u_e(p_2) = \sqrt{s} (0, -i, -1, 0) \\ J_R^{\mu} &= \bar{v}_e(p_1)\gamma^{\mu}\omega_+u_e(p_2) = \sqrt{s} (0, i, -1, 0), \end{aligned}$$

which is orthogonal with respect to the total initial-state momentum  $p_1 + p_2 = p_+ + p_-$ .

Exploiting the various properties of the polarization vectors and electron-positron currents, we end up with the following leading non-local contributions to the right- and left-handed transverse amplitudes at high energies:

$$\begin{aligned} \mathcal{M}_R &\approx (ie)^2 \beta \sin \theta \left[ \frac{s}{2} \tilde{\Sigma}'_2(M_W^2) \right] \frac{s}{D(s)} \left\{ \frac{s}{c_w^2} \tilde{\Sigma}_3(s) + M_Z^2 \left[ 1 + \tilde{\Sigma}_5(s) + \tilde{\Sigma}_6(s) \right] \right\} \\ \mathcal{M}_L &\approx (ie)^2 \beta \sin \theta \left[ \frac{s}{2} \tilde{\Sigma}'_2(M_W^2) \right] \frac{s}{D(s)} \left\{ -\frac{s}{2s_w^2} \left[ 1 + \tilde{\Sigma}_1(s) - \frac{s_w^2}{c_w^2} \tilde{\Sigma}_3(s) \right] \right. \\ &\quad \left. + M_Z^2 \left[ 1 + \tilde{\Sigma}_5(s) + \tilde{\Sigma}_6(s) \right] \right\}. \end{aligned} \tag{86}$$



A few remarks are in order here. First of all, the matrix elements  $\mathcal{M}_{R,L}$  given in Eq.(86) are valid only if both  $W$  bosons have the same transverse helicity. The matrix elements vanish if the  $W$  bosons have opposite helicity. Second, the factor  $s \tilde{\Sigma}'_2(M_W^2)/2$  is the leading high-energy component of the non-local triple gauge-boson vertex of Eq.(56), which has to be contrasted with the corresponding factor  $-1$  for the local triple gauge-boson vertex. The derivative  $\tilde{\Sigma}'_2(M_W^2)$  originates from the typical non-local expression

$$\frac{\tilde{\Sigma}_2(p_-^2) - \tilde{\Sigma}_2(p_+^2)}{p_-^2 - p_+^2} \xrightarrow{p_{\pm}^2 \rightarrow M_W^2} \tilde{\Sigma}'_2(M_W^2). \quad (87)$$

Since  $D(s) \propto s^2$  at high energies [see Eq.(53)],  $\mathcal{M}_L$  will have an incorrect high-energy behaviour, growing with  $s$  as a result of the non-local triple gauge-boson factor  $s \tilde{\Sigma}'_2(M_W^2)/2$ . [Note that this is not the case for  $\mathcal{M}_R$  in view of the fact that  $\tilde{\Sigma}_3(s)$  vanishes at high energies.] On the basis of this observation we conclude that the BBC approach has a problem with high-energy unitarity.

## References

- [1] M. W. Gr unewald *et al.*, hep-ph/0005309;  
E. Accomando *et al.* [ECFA/DESY LC Physics Working Group Collaboration], Phys. Rept. **299** (1998) 1 [hep-ph/9705442].
- [2] E. N. Argyres *et al.*, Phys. Lett. B **358** (1995) 339 [hep-ph/9507216].
- [3] W. Beenakker *et al.*, Nucl. Phys. B **500** (1997) 255 [hep-ph/9612260].
- [4] G. Passarino, Nucl. Phys. B **574** (2000) 451 [hep-ph/9911482].
- [5] E. Accomando, A. Ballestrero and E. Maina, Phys. Lett. B **479** (2000) 209 [arXiv:hep-ph/9911489].
- [6] R. G. Stuart, Phys. Lett. B **262** (1991) 113;  
A. Aeppli, G. J. van Oldenborgh and D. Wyler, Nucl. Phys. B **428** (1994) 126 [hep-ph/9312212].
- [7] W. Beenakker, F. A. Berends and A. P. Chapovsky, Nucl. Phys. B **548** (1999) 3 [hep-ph/9811481].
- [8] A. Denner, S. Dittmaier, M. Roth and D. Wackeroth, Nucl. Phys. B **587** (2000) 67 [hep-ph/0006307].

- [9] K. Melnikov and O. I. Yakovlev, Nucl. Phys. B **471** (1996) 90 [hep-ph/9501358];  
W. Beenakker, A. P. Chapovsky and F. A. Berends, Phys. Lett. B **411** (1997) 203 [hep-ph/9706339] and Nucl. Phys. B **508** (1997) 17 [hep-ph/9707326];  
A. Denner, S. Dittmaier and M. Roth, Nucl. Phys. B **519** (1998) 39 [hep-ph/9710521] and Phys. Lett. B **429** (1998) 145 [hep-ph/9803306].
- [10] W. Beenakker, F. A. Berends and A. P. Chapovsky, Nucl. Phys. B **573** (2000) 503 [hep-ph/9909472].
- [11] M. E. Peskin and T. Takeuchi, Phys. Rev. D **46** (1992) 381.
- [12] P. Sikivie, L. Susskind, M. B. Voloshin and V. I. Zakharov, Nucl. Phys. B **173** (1980) 189.
- [13] J. A. Vermaseren, “The Symbolic manipulation program FORM,” KEK-TH-326; <http://www.nikhef.nl/~form/FORMdistribution/index.html>
- [14] A. Denner, Fortsch. Phys. **41** (1993) 307.
- [15] R. Mertig, M. Bohm and A. Denner, Comput. Phys. Commun. **64** (1991) 345.
- [16] J. L. Hewett, hep-ph/9810316.
- [17] A. Kanaki, Ph.D. thesis, in preparation.
- [18] F. A. Berends, C. G. Papadopoulos and R. Pittau, Comput. Phys. Commun. **136** (2001) 148 [hep-ph/0011031].
- [19] A. Kanaki and C. G. Papadopoulos, Comput. Phys. Commun. **132** (2000) 306 [hep-ph/0002082];  
A. Kanaki and C. G. Papadopoulos, “HELAC-PHEGAS: Automatic computation of helicity amplitudes and cross sections”, hep-ph/0012004.
- [20] G. J. van Oldenborgh, Comput. Phys. Commun. **66** (1991) 1.
- [21] K. Hagiwara et al., Phys. Rev. **D66**, 010001 (2002).
- [22] G. Passarino, Nucl. Phys. B **578** (2000) 3 [hep-ph/0001212].
- [23] A. Sirlin, Phys. Rev. Lett. **67** (1991) 2127 and Phys. Lett. B **267** (1991) 240.